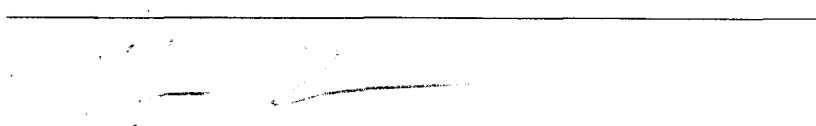


BIOSORPTION OF LEAD BY CITRUS PECTIN AND PEELS  
IN AQUEOUS SOLUTION

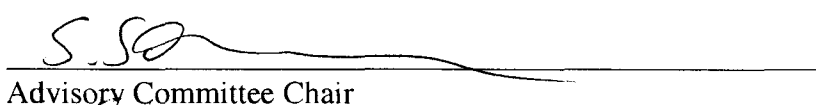
By

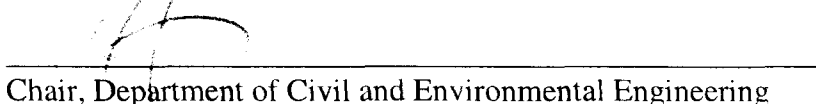
Ankit Balaria

RECOMMENDED:





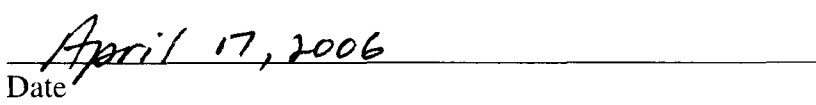
  
Advisory Committee Chair

  
Chair, Department of Civil and Environmental Engineering

APPROVED:

  
Dean, College of Engineering and Mines

  
Dean of the Graduate School

  
Date

BIOSORPTION OF LEAD BY CITRUS PECTIN AND PEELS  
IN AQUEOUS SOLUTION

A

THESIS

Presented to the Faculty

of the University of Alaska Fairbanks

in Partial Fulfillment of the Requirements

for the Degree of

MASTER OF SCIENCE

By

Ankit Balaria, B. Tech.

Fairbanks, Alaska

May 2006

BIOSCI  
OK  
208  
P4  
L25  
-2006

## Abstract

Biosorption of heavy metal ions by different pectin rich materials such as waste citrus peels is emerging as a promising technique for metallic contaminant removal. While binding rate and capacity of citrus peels were previously investigated, there is a lack of mechanistic information about Pb-citrus pectin/peels interaction mechanisms. Present research focused on evaluating this binding mechanism by corroborating macroscopic studies with spectroscopic techniques. Citrus pectins of two different methoxylation degrees and orange peels were characterized using potentiometric titrations and Fourier transform infrared (FTIR) spectroscopy. Binding mechanisms were evaluated using molecular scale FTIR analyses. The effects of particle size, pH, co-ion presence, and background electrolyte concentrations were also investigated for biosorption of Pb by orange peels.

Both citrus pectin and orange peels reached their sorption equilibrium within 45 minutes. The maximum uptake capacity for orange peels was found to be 2.32 mmol/g. Citrus peels have very similar FTIR spectra to citrus pectin, suggesting that they have similar functional groups and pectin can be used as a model for citrus peels. Furthermore, carboxylic acid groups were found to be responsible for binding of Pb by citrus pectin and orange peels.

## Table of Contents

	Page
<b>Signature Page</b> .....	i
<b>Title Page</b> .....	ii
<b>Abstract</b> .....	iii
<b>Table of Contents</b> .....	iv
<b>List of Figures</b> .....	vii
<b>List of Tables</b> .....	xi
<b>List of Appendices</b> .....	xii
<b>Acknowledgements</b> .....	xiii
<b>Chapter 1: Introduction</b> .....	1
1.1 Background.....	1
1.1.1 Lead in the Environment.....	1
1.1.2 Lead Pollution Control.....	2
1.1.3 Biosorption.....	3
1.2 Hypotheses and Objectives.....	6
<b>Chapter 2: Literature Review</b> .....	8
2.1 Sorbent Selection and Preparation.....	8
2.2 Characterization of Sorbent.....	11
2.3 Kinetic Studies.....	13
2.4 Effects of Environmental Conditions.....	16
2.5 Biosorption Isotherms.....	17

	Page
2.6 Regeneration of Sorbent.....	20
<b>Chapter 3: Materials and Methods.....</b>	<b>21</b>
3.1 Material Selection.....	21
3.2 Preliminary Experiments.....	22
3.3 Sorbent Characterization.....	23
3.3.1 Potentiometric Titrations.....	23
3.3.2 FTIR Experiments.....	25
3.4 Binding Evaluation.....	25
3.4.1 Kinetic Experiments.....	26
3.4.2 Effect of Environmental Conditions.....	26
3.4.3 Isotherms.....	27
3.4.4 pH Variability Study.....	27
3.4.5 Mechanism Investigation.....	28
3.4.6 Experimental Error Considerations.....	28
3.4.7 Modeling Error Analysis.....	29
<b>Chapter 4: Results and Discussion.....</b>	<b>30</b>
4.1 Characterization of Sorbents.....	30
4.1.1 Sorbent Charge.....	30
4.1.2 Sorbate Functional Groups.....	33
4.2 Biosorption Studies.....	35
4.2.1 Batch Kinetics.....	35

	Page
4.2.2 Effect of Environmental Conditions.....	46
4.2.3 Biosorption Isotherm.....	51
4.2.4 pH Variability Study.....	56
4.2.5 Spectroscopic Studies.....	59
<b>Chapters 5: Conclusions and Recommendations.....</b>	<b>63</b>
5.1 Conclusions.....	63
5.2 Recommendations for Future Work.....	64
<b>References.....</b>	<b>65</b>
<b>Appendices.....</b>	<b>75</b>

## List of Figures

	Page
Figure 1.1: Structure of alginate and pectin (Genialab 2002)	5
Figure 2.1: Schematic diagram of biosorption process	20
Figure 3.1: Dried and ground orange peels donated by Biotex Corporation	21
Figure 3.2: Solubility diagram for precipitation of $\text{Pb}(\text{OH})_2$ at 25 °C and a background electrolyte concentration of 0.01 M $\text{NaNO}_3$ (Circle indicates reaction conditions)	23
Figure 4.1: Potentiometric titrations of LM and HM pectins at a background electrolyte concentration of 0.01 M $\text{NaNO}_3$	31
Figure 4.2: Potentiometric titrations of LM and HM pectins at a background electrolyte concentration of 0.1 M $\text{NaNO}_3$	32
Figure 4.3: Potentiometric titrations orange peels at a background electrolyte concentration of 0.01 M $\text{NaNO}_3$	32
Figure 4.4: FTIR spectra of LM pectin, HM pectin, orange peels, and protonated orange peels	34
Figure 4.5: Pb-LM pectin kinetic data modeling using a pseudo second-order model	37
Figure 4.6: Pb-HM pectin kinetic data modeling using a pseudo second-order model	37

Figure 4.7: Linear fitting of Pb-pectin kinetic data using a pseudo first-order model	38
Figure 4.8: Linear fitting of Pb-LM pectin kinetic data using a pseudo second-order model	38
Figure 4.9: Linear fitting of Pb-HM pectin kinetic data using a pseudo second-order model	39
Figure 4.10: Pb-peels (< 0.6 mm) kinetics modeling using a pseudo second-order model	40
Figure 4.11: Pb-peels (0.6-1.0 mm) kinetics modeling using a pseudo second-order model	41
Figure 4.12: Pb-peels (1.0-3.0 mm) kinetics modeling using a pseudo second-order model	41
Figure 4.13: Pb-peels kinetic data fitting using a linearized pseudo first-order model	42
Figure 4.14: Pb-peels (<0.6 mm) kinetic data fitting using a linearized pseudo second-order model	43
Figure 4.15: Pb-peels (0.6-1.0 mm) kinetic data fitting using a linearized pseudo second-order model	43
Figure 4.16: Pb-peels (1.0-3.0 mm) kinetic data fitting using a linearized pseudo second-order model	44

Figure 4.17: Effect of pH on biosorption of 0.1 mM Pb by 0.1 g/L peels at room temperature	48
Figure 4.18: Effect of pH on biosorption of 0.1 mM Pb by 1 g/L peels at room temperature	48
Figure 4.19: Effect of co-ions on biosorption of 0.1 mM Pb by 0.1 g/L peels at room temperature and pH 5	49
Figure 4.20: Effect of co-ions on biosorption of 0.1 mM Pb by 1 g/L peels at room temperature and pH 5	49
Figure 4.21: Effect of ionic strength (NaNO <sub>3</sub> as background electrolyte) on biosorption of 0.1 mM Pb by 0.1 g/L peels at room temperature and pH 5	50
Figure 4.22: Effect of ionic strength (NaNO <sub>3</sub> as background electrolyte) on biosorption of 0.1 mM Pb by 0.1 g/L peels at room temperature and pH 5	50
Figure 4.23: Biosorption isotherm modeling for Pb binding by orange peels (size 0.6 mm to 1.0 mm) at room temperature and pH 5	54
Figure 4.24: Pb-peels isotherm data fitting using a linearized Langmuir model	55
Figure 4.25: Pb-peels isotherm data fitting using a linearized Freundlich model	55
Figure 4.26: pH variability study for Pb sorption by citrus pectin and peels	58
Figure 4.27: H <sup>+</sup> released ( $\Delta H$ ) on incremental addition of Pb to the sorbent solution	58

Figure 4.28: FTIR results for Pb binding by HM pectin	60
Figure 4.29: FTIR results for Pb binding by LM pectin	61
Figure 4.30: FTIR results for Pb binding by protonated orange peels	62
Figure 4.31: FTIR results for Pb binding by orange peels at different Pb concentrations: 0.1 mM Pb-peels (Pb(II)-peels) and 0.01 mM Pb-peels (low Pb(II)-peels)	63
Figure B.1: Kinetics of binding of $10^{-3}$ M Pb by 1g/L LM pectin at room temperature and with 0.01 M $\text{NaNO}_3$ as background electrolyte	76
Figure B.2: Effect of initial Pb concentrations on binding of Pb by 1g/L LM pectin at pH 8, room temperature, and with 0.01 M $\text{NaNO}_3$ as background electrolyte	77
Figure B.3: Effect of pectin concentration on binding of $10^{-3}$ M Pb by LM pectin at pH 8, room temperature, and with 0.01 M $\text{NaNO}_3$ as background electrolyte	77
Figure B.4: Effect of ionic strength on binding of $10^{-3}$ M Pb by 1g/L LM pectin at pH 8 and room temperature	78
Figure B.5: Effects of presence of co-ions on binding of $10^{-3}$ M Pb by 1 g/L LM pectin at pH 8, room temperature, and with 0.01 M $\text{NaNO}_3$ as background electrolyte	78

**List of Tables**

	Page
Table 2.1: Characteristic components of citrus pectin (Dronnet et al., 1996)	11
Table 4.1: Total surface charge of sorbents as determined by potentiometric titrations at pH 5 and a background electrolyte concentration of 0.01 M NaNO <sub>3</sub>	33
Table 4.2: Second-order kinetic parameters for Pb gelation with pectin	39
Table 4.3: Second-order kinetic parameters for Pb biosorption by orange peels	45
Table 4.4: Equilibrium parameters for Langmuir and Freundlich isotherm models	56
Table C.1: Duplicate Experiments and Sampling	79

**List of Appendices**

	Page
Appendix A: List of Symbols and Acronyms	75
Appendix B: Preliminary Experimental Results	76
Appendix C: Duplicate Experiments and Sampling	79

## **Acknowledgements**

First of all, I would like to thank my brother, whose motivation and support has always encouraged me in every endeavor of my life. I am highly grateful to my advisor Dr. Silke Schiewer, who was always available for guidance and suggestions. I would like to acknowledge my advisory committee members Dr. Thomas P. Trainor, Dr. Daniel M. White, and Dr. David L. Barnes for contributing their valuable time for my research. I am thankful to all my teachers who introduced me to numerous disciplines of environmental engineering.

I would like to thank Santosh, Kunal, Hrishikesh, Kim, Hong, Shawna, and Shane for their help and co-operation during the experiments and data analysis. I would like to present my gratitude to the Water and Environmental Research Center (WERC) and Civil and Environmental Engineering Department (CEE) for providing me with the instrumentation, lab facilities, and funding in form of a teaching assistantship. I would also like to acknowledge Biotex Corporation for providing the orange peels and United States Geological Survey (USGS) and United States Department of Agriculture (USDA) for funding the research.

## **Chapter 1**

### **Introduction**

#### **1.1 Background**

##### **1.1.1 Lead in the Environment**

Lead (Pb) is a bluish-gray metal found in small amounts in the earth's crust (ATSDR, 2005). It has a melting point 327.5 °C, which is much lower than for other easily available metals e.g. iron: 1535.0 °C and copper: 1083.0 °C. Moreover, metallic lead is resistant to corrosion and readily forms alloys with other metals. The ease with which lead can be molded and shaped into a required form and its high durability make it an important construction material. Lead has been extensively mined and used in human societies over thousands of years. Lead pipes were used for water supply even during the Roman Empire. As time proceeded, other uses for lead were implemented such as in batteries, petroleum products, ammunitions, paints, cosmetics, and even wine as a sweetening agent (Grandjean, 1975).

Production and use of lead and lead based products lead to its release into the environment. Lead is released either as lead-rich aqueous effluent or emitted with fumes and dust into the air (Harrison and Laxen, 1981). Once lead enters the environment, it does not break down, but undergoes transformations by sunlight, air, and water. When lead is released to the air, it may travel long distances before settling on the ground and onto water bodies. Once deposited, it usually remains in the upper layer of soil and can be

transported to surface waters. When it enters the natural aquatic systems, it becomes mobile and bio-available and subsequently a source for human exposure (ATSDR, 2005).

### **1.1.2 Lead Pollution Control**

Lead can affect almost every organ and system of a human body. At high levels, lead may increase reaction time, cause weakness in fingers, wrists, ankles, and possibly affect memory. Lead may also cause anemia and damage the male reproductive system. It has proved deadly to exposed children (Harrison and Laxen, 1981). Based on toxicity and high possibility of exposure of lead, the U.S. Environmental Protection Agency has listed it as a priority pollutant, and its fate and transport in atmospheric and aquatic systems has become one of the primary concerns of environmental science (US EPA, 1989).

In order to reduce human exposure to lead, the use of lead in gasoline has been banned by the United States government since January 1, 1996. Lead is also no longer used in paints, water pipes, solders, or construction materials. The battery industry is the largest consumer of lead and it employs 97% recycling in order to reduce primary production of lead i.e. the production by direct mining in form of its ores. Alaska and Missouri are the two major states in the United States responsible for most of the primary production of lead at present (ATSDR, 2005).

Because of reduced use of lead based petroleum products which contribute to lead release to the atmosphere, its atmospheric deposition onto soil and surface waters is no

longer a major concern. The largest source of aqueous lead pollution is now waste water from battery, electroplating, and other related industries. These industries are required to meet certain criteria for the amount of lead in their waste streams prior to discharge to natural water bodies.

Traditional methods for treatment of lead in aqueous waste streams include coagulation/precipitation, reverse osmosis, electrochemical techniques, and ion exchange (Volesky, 1990). Precipitation followed by coagulation has been extensively employed because of its easy operation and low cost. However, this process usually produces large volumes of toxic sludge containing small amounts of the heavy metal lead, which is very difficult to recycle and reuse. Furthermore, the quality of the effluent stream is not good enough to meet the present stringent criteria. Processes such as reverse osmosis, electrochemical methods, and ion exchange provide an effective removal of lead from the waste streams, but they are very expensive.

### **1.1.3 Biosorption**

Biosorption, sorption onto biological materials, has emerged as a potential alternative method for aqueous removal of transition and heavy metals such as lead (Volesky, 1990). It is a process that involves binding of the metal ions by living (Pagnanelli et al., 2000) or dead (Cossich et al., 2002; Atkinson et al., 1998; Dronnet et al., 1997) biological materials. It is a promising technique because very cheap materials such as industrial waste products or naturally abundant biomass can be employed for the

purpose. These biosorbents can be obtained almost free of charge as producers often pay for their disposal. The only considerable cost for these raw materials is the cost of drying and transportation (Atkinson et al., 1998).

Biosorption is a highly efficient process, considering the fact that it can remove metal ions present in very high to very low concentration with a great degree of overall removal. A number of researchers have studied different biological materials for removal of heavy metal ions such as polymerized corncob (Henderson et al., 1997), moss (Low and Lee, 1987), hulls and bran (Marshall et al., 1993), and brown algae (Davis et al., 2003; Cossich et al., 2002; Chen and Wang, 2001). Pagnanelli et al. (2000) studied biosorption of lead and other heavy metals by a living culture of *Arthrobacter sp.* The results were promising but it is difficult and relatively expensive to maintain suitable environmental conditions for microbial cultures in water containing lead and other toxic metal ions. It is for this reason that passive uptake of metal ions by a variety of non-living biosorbent materials has been studied extensively.

Many studies have been conducted to understand effects of environmental conditions on binding rate and capacity of heavy metal ions by brown algae (Davis et al., 2003; Cossich et al., 2002; Chen and Wang, 2001). Brown algae represent a good biosorbent due to the presence of alginate in the cell wall which contains carboxylic groups. Due to deprotonation at certain pH values, these carboxylic groups become negatively charged and ready to bind with positive metal ions in aqueous solutions.

Pectin is a biopolymer with a structure very similar to alginate (Figure 1.1). It is present in high quantities in a number of fruits and vegetables such as citrus fruits, sugar beets, apples etc. Only a few researchers have studied binding of heavy metal ions by pectin with changing environmental conditions such as pH, ionic strength, sorbate/sorbent concentration and temperature (Debbaudt et al., 2001; Dronnet et al., 1996; Ferreira and Gschaider, 2001; Harel et al., 1998; Kartel et al., 1998; Kohn, 1987; Racape et al., 1989; Sergushchenko et al., 2003; Yano and Inoue, 1997). Although these studies provide some insight for the binding rate and capacity for pectin, there is a lack of information about the binding mechanisms. A study of the binding mechanisms for Pb-pectin interactions can be helpful to better understand the process chemistry.

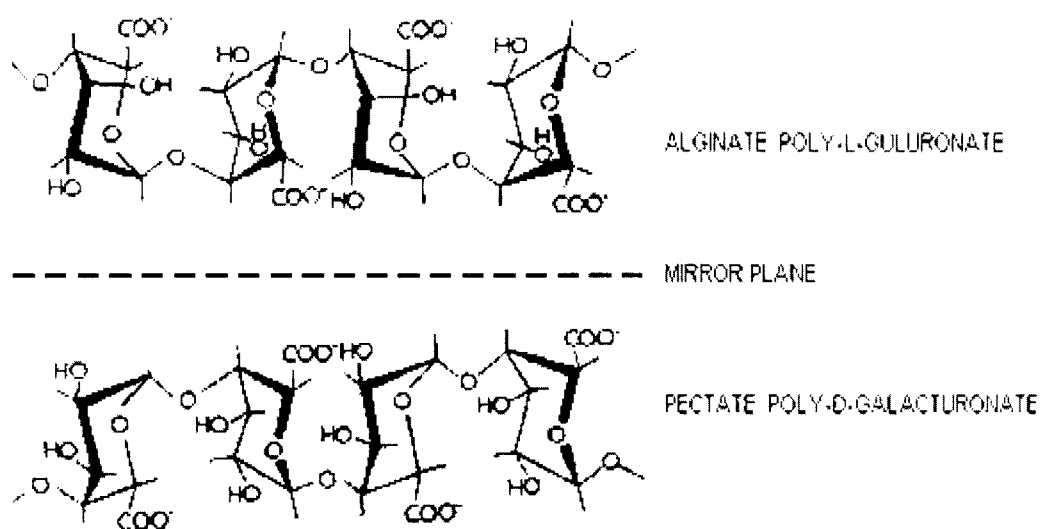


Figure 1.1: Structure of alginate and pectin (Genialab, 2002)

It is also important to study citrus peels as biosorbents for heavy metal ions such as lead because they are very cheap and rich in pectin. The total amount of orange production per year in the USA is approximately 10,000,000 tons. About 50% of the total mass of citrus fruits results in waste, which includes mainly peels and fibers. Only about 15 % - 20 % of this waste is used productively, such as for pectin production, leaving a vast amount of remaining waste to handle. Dried citrus peels for pectin production are sold for \$300-600/ton (Vincent, 2001), while presently ion exchange resins cost from \$30,000 to 50,000/ton. Some preliminary research has suggested that biosorption of lead by citrus peels is efficient and can be utilized with good possibilities of sorbent regeneration by desorption of the metal ions (Ajmal et al., 2000; Annadurai et al., 2003; Inoue et al., 2002; Jumle et al., 2002; Senthilkumaar et al., 2000). Determining the lead sorption rate and capacity and understanding the involvement of pectin in sorption by citrus peels is important for commercial use of this sorbent material.

## **1.2 Hypotheses and Objectives**

This research is conducted in order to understand the biosorption of Pb by citrus pectin and citrus peels. The hypotheses for the research work are

- *Biosorption of lead by orange peels is similarly fast and efficient as ion exchange resins.*
- *Carboxylic acid groups play a dominant role in lead binding by citrus pectin and orange peels.*

To test these hypotheses and to predict the responsible factors for the metal ions sorption, the project objectives included

- To characterize the sorbent materials with respect to their total surface charge in aqueous solution using potentiometric titrations and understand the effect of methoxylation degree on surface charge of citrus pectin.
- To determine the main organic functional groups of citrus pectin and peels using Fourier Transform Infrared Spectroscopy.
- To model kinetics of Pb binding by high and low methoxylated citrus pectins.
- To understand effects of mass transfer on biosorption of Pb by citrus peels by comparing kinetic results of citrus peels of different sizes.
- To study the effect of environmental conditions such as pH, co-ions, and ionic strength on overall binding by citrus peels.
- To conduct isotherm experiments in order to quantify the biosorption of Pb by citrus peels.
- To study changes in pH of solutions containing citrus pectin/peels with addition of Pb in order to understand solution chemistry.
- To conduct spectroscopic analyses of the sorption samples obtained for Pb binding by citrus peels/pectin in order to investigate the functional groups contributing to biosorption by these materials.

## Chapter 2

### Literature Review

#### 2.1 Sorbent Selection and Preparation

A number of pectin-rich biological materials have been studied for their metal binding abilities. These materials range from cheap, naturally occurring materials such as aquatic ferns (Cohen-Shoel et al., 2002) and tree barks (Gloaguen and Morvan, 1997), to waste products of food industries such as apple waste (Lee et al., 1999; Maranon and Sastre, 1992), sugar beet pulp (Dronnet et al., 1996; Gerente et al., 2000; Reddad et al., 2002), and orange peels (Ajmal et al., 2000; Annadurai et al., 2003; Inoue et al., 2002; Jumle et al., 2002; Senthilkumaar et al., 2000).

Cohen-Shoel et al. (2002) studied involvement of pectin in biosorption of the divalent positive metal ion Sr by the aquatic fern, *Azolla*. They performed methylation of the sorbent material by treating with absolute methanol and HCl. The methylated biomass was found to be of reduced binding capacity as compared to the untreated one.

Gloaguen and Morvan (1997) investigated removal of divalent positive ions Pb, Zn, Cr, Fe, and Cu by using some commonly available tree barks such as *Picea abies*, *Pinus sylvestris*, *Pseudotsuga manziesii*, *Larix kaempferi*, *Tectona grandis*, and *Azalia africana*. These barks were air-dried, ground, sieved and then chemically treated with dilute formaldehyde in acidic conditions in order to polymerize and insolubilize

pectin/tannin compounds. Pectin was found to be an important component responsible for binding of metal ions.

Maranon and Sastre (1992) studied binding of Cu, Zn, and Ni by waste from the apple juice processing industry. They used chemical modification of the sorbent by introduction of phosphate groups as a cross-linking agent followed by protonation. Chemically modified apple waste was found to have a higher binding capacity than the untreated waste. The waste was also ready for re-use after metal elution with hydrochloric acid. Lee and Yang (1997) also studied apple residue for binding of Cu ions and found similar promising results.

Dronnet et al. (1997) studied binding of the divalent positive metal ions Pb, Ca, Cd, Cu, Ni, and Zn by sugar beet pulp. They treated the dried pulp with boiling ethanol and filtered it in order to inactivate endogenous enzymes and discard residual monomers and oligomers. The resulting pulp was dried by solvent exchange and then air for final use as biosorbent for the experiment. The resulting pulp was treated with acid in order to protonate the sorbent. Reddad et al. (2002) also used dried, ground, washed, and again dried sugar beet pulp for binding experiments with Ni and Cu. They also modified the pulp by both acid and base extractions. Gerente et al. (2000) investigated raw, washed, and acid washed forms of sugar beet pulp for binding of Cu, Ni, and Pb ions.

Annadurai et al. (2003) studied binding of divalent positive metal ions Pb, Ni, Zn, Cu, and Co by banana and orange peels. These peels were cut into small pieces, dried, crushed, washed with double distilled water, and air dried at 100 °C before use. Results suggested that orange peels are better at adsorbing the metal ions compared to banana peels. Ajmal et al. (2000), Inoue et al. (2002), Jumle et al. (2002), and Senthilkumaar et al. (2000) also studied the binding of various metal ions by orange peels in raw or protonated forms and found promising results.

Pectin obtained from various sources has also been studied with respect to binding capacity and effects of environmental conditions. Kohn (1987) studied binding of Ca, Cd, Cu, Pb, Sr, and Zn by pectin for use in medicinal purposes. Sergushchenko et al. (2003) compared the sorption capacity of pectin obtained from sea grass *Zostera marina* with other sorbent materials. Yano and Inoue (1997) and Racape et al. (1989) studied effects of amidation of pectin on metal binding. Debbaudt et al. (2001) and Ferreira and Gschaider (2001) studied Cu and Pb binding by pectin used in pelleted form, whereas Harel et al. (1998) used pectin for metal ion binding in form of beads. Dronnet et al. (1996) performed comparative evaluation of metal ion binding by citrus and sugar-beet pectin. Kartel et al. (1999) compared citrus pectin, sugar-beet pectin, and apple pectin with respect to metal binding. These studies suggest that citrus pectin is the most efficient pectin for binding of metal ions because of the absence of acetyl groups which have lower affinity towards metal ions as compared to carboxylic groups.

Present work utilized citrus peels for biosorption of Pb. Citrus peels were used because of their high pectin content. These peels were used without chemical pretreatment in order to maintain the originality of the material. Citrus pectins with high and low of methoxylation degrees (64% and 9%) were also used to investigate the binding mechanism with simpler model substances.

## 2.2 Characterization of Sorbent

It is important to characterize the sorbent material before conducting any binding experiments. Dronnet et al. (1996) conducted an extensive characterization of citrus pectin which is presented in Table 2.1.

Table 2.1: Characteristic components of citrus pectin (Dronnet et al., 1996)

Component	Quantity, mg/g
Galacturonic acid	911
Rhamnose	11
Fucose	traces
Arabinose	15
Xylose	1
Mannose	traces
Galactose	38
Glucose	3

They characterized citrus pectin with a degree of methoxylation (i.e. % methoxylated carboxylic groups in the pectin structure) of 54% and a degree of acetylation of 0% (i.e. % acetylated carboxylic groups in the pectin structure). The molecular weight of this pectin was found to be  $171 \times 10^3$  and the cation exchange capacity was 2.38 meq/g.

Potentiometric titration is a good way to evaluate the total charge imparted to the solution in which the sorbent material is suspended (Stumm and Morgan, 1970). Based on the changes in pH due to the addition of acid or base the total solution charge (equivalents) imparted by the sorbent material can be determined using the electro-neutrality equation of the solution. The present study used this method to compare the charges of high and low methoxylated pectins and the citrus peel under investigation. This study was also performed at different background electrolyte concentrations in order to study the effect of ionic strength on the surface charge availability.

Potentiometric titrations have also been used previously to characterize  $pK_a$  values of the functional groups present in biological materials such as brown seaweeds (Yun et al., 2001) and sugar beet pulp (Reddad et al., 2002). Although potentiometric titration is a good method to predict functional groups by comparing the  $pK_a$  value which correspond to the points of inflection of the curves, its results can not be trusted with certainty (Reddad et al., 2002). For this reason we used FTIR spectroscopy to characterize the functional groups of the sorbent materials used in the present study.

A number of researchers have characterized different kinds of pectin with FTIR (Gnanasambandam and Proctor, 1999; Monsoor et al., 2001; Copikova et al., 2001). We compared the results of our studies with these previous investigations to predict the functional groups in the high and low methoxylated citrus pectins and citrus peels.

### 2.3 Kinetic Studies

Many researchers have studied kinetics of metal ion sorption for various biosorbent materials. The sorption rates were found to be of pseudo first-order and pseudo second-order for different biosorbent materials and different environmental conditions of pH, ionic strength, temperature, initial metal ions concentration, and sorbent loading.

The pseudo first-order model assumes that the rate of change of surface site concentration is proportional to the amount of remaining unoccupied surface sites. This model can be described as:

$$\frac{dq}{dt} = k_1(q_e - q) \quad (2.1)$$

where  $q$  and  $q_e$  are adsorbed amounts (in mg/g) at time  $t$  (in min) and equilibrium, respectively and  $k_1$  (in  $\text{min}^{-1}$ ) is the first-order adsorption rate constant (also referred to as the Lagergren rate constant). This model can be simplified to the linear form as:

$$\log(q_e - q) = \log q_e - \frac{k_1}{2.303} t \quad (2.2)$$

The pseudo second-order model assumes that the rate of change of surface site concentration is proportional to the square of amount of remaining surface sites. This model can be described as:

$$\frac{dq}{dt} = k_2(q_e - q)^2 \quad (2.3)$$

where  $q$  and  $q_e$  are adsorbed amounts (in mg/g) at time  $t$  (in min) and equilibrium, respectively and  $k_2$  (in g/meq-min) is the second-order adsorption rate constant. This model can be linearized as:

$$\frac{t}{q} = \frac{1}{k_2 q_e^2} + \frac{t}{q_e} \quad (2.4)$$

Debbaudt (2001) investigated binding of Pb by pectin with respect to time and found that its maximum removal (about 50% of total Pb) was achieved in 1 h with pH being fixed between pH 4 and 5. Ajmal et al. (2000) studied kinetics of Ni sorption by orange peels and modeled the rate using first-order kinetics. They studied the sorption rates at three different temperatures: 30 °C, 40 °C, and 50 °C. The sorption capacity increased with an increase in temperature, but the time course followed the same pattern with maximum sorption achieved in around 2 h. They used a first-order model for fitting the kinetic data and obtained straight line plots of  $\log(q_e - q)$  vs.  $t$ , suggesting that the model can be used for metal ion sorption by citrus peels.

Reddad et al. (2002) studied Ni and Cu biosorption by pectin rich sugar beet pulp and found that kinetics could be fitted well by a second-order rate model. Antunes et al. (2003) investigated copper removal by the brown seaweed *Sargassum sp.* and achieved equilibrium in 30 min. They found an increase in sorption capacity with increase in pH. The authors compared a pseudo first-order Lagergren model and pseudo second-order model for kinetic modeling and concluded that sorption followed pseudo second-order kinetics. Hashim and Chu (2004) studied kinetics of Cd biosorption by brown, red, and green seaweeds and found that 90% or more of biosorption took place within 30-40 minutes of contact time. They also fitted the kinetic data with both first- and second-order kinetic models using a nonlinear least-squares method to determine the rate constant of the two models. They found that the first-order kinetic model was able to simulate the entire concentration-time profile. The second-order kinetic model was able to simulate the initial stage of high and rapid uptake, but underestimated metal ion uptake during the stage of slow approach to equilibrium for longer times.

Volesky (2003) suggested that for batch dynamics, kinetics of the sorption reaction itself have to be distinguished from a time based study of the sorption process, as the latter involves additional phenomena such as intra-particle diffusion. Intra-particle diffusion is the slow diffusion of metal ions into small pores on the sorbent surface and can be a rate determining factor in many biosorption cases, where sorbents are highly porous and retain their shape in aqueous solution for longer times.

## 2.4 Effects of Environmental Conditions

Both binding rate and capacity for biosorption of metal ions depend on several environmental conditions including pH, temperature, ionic strength, initial metal ions concentration, co-ion presence, and sorbent properties. This section summarizes previous research for biosorption of metal ions at different environmental conditions.

Annadurai et al. (2003) studied the effect of pH on binding of the metal ions Pb, Ni, Zn, Cu, and Co and found that metal uptake increases with increasing pH due to competition of metal ions with protons at lower pH values. Cohen-Shoel et al. (2002) studied pH effects on biosorption of Sr by aquatic fern *Azolla* and found optimal binding at high pH values indicating de-esterification of pectin and exposure of additional available carboxyl groups. They found 95% removal at pH 7 and 99% removal at pH 10. These removal efficiencies are impressive, but they cannot be attributed only to the biosorption. Rather a direct metal precipitation is very possible at such high pH values, which could be contributing to the metal removal from solution.

The effect of temperature on biosorption is highly sorbent specific. Cossich et al. (2002) found that for biosorption of Cr on *Sargassum sp.* biomass (a marine alga), a temperature increase from 20 °C to 30 °C caused no significant change in total uptake but for an increase in temperature from 30 °C to 40 °C, the sorption capacity decreased. These results are contrary to results of Ajmal et al. (2000); they found an increase in

sorption capacity with increase in temperature from 30 °C to 50 °C for biosorption of Ni on orange peels, indicating the sorption reaction to be endothermic.

Lee and Yang (1997) studied Cu binding by pectin rich apple waste and found that ionic strength did not cause significant differences in metal ion binding capacity. They also found that the presence of co-ions such as lead decreased the removal of Cu due to competition. The presence of ligands such as EDTA and ammonia also reduced the metal ion removal efficiency due to formation of metal ligand complexes in solution. Hashim and Chu (2004) found that the presence of background cations such as sodium, potassium, and magnesium and anions such as chloride, nitrate, sulfate, and acetate had no significant effect on cadmium biosorption by the *Sargassum* biomass. However, cadmium uptake was inhibited in the presence of calcium ions of the same concentration.

The effect of sorbent particle size had been investigated by Cossich et al. (2002). They used seaweeds of two different particle sizes having the same thickness (i.e. same diffusion distance) and found no significant effect of particle size on total sorption capacity. Gloaguen et al. (1997) studied the effects of grain size of tree barks on sorption of metal ions and concluded that smaller grain size sorbents had higher sorption capacity.

## **2.5 Biosorption Isotherms**

In order to propose the use of biological material as a biosorbent, it is important to determine the binding capacity of metal ions for the biosorbent. This binding capacity can

be determined by modeling the sorption equilibrium using sorption isotherms. Volesky (2003) summarized seven models which could be used to mathematically describe the single component biosorption systems (which are the most commonly studied systems). The most commonly used are the two-parameter Langmuir and Freundlich isotherms, due to their simplicity and ease of interpretability.

The Langmuir model assumes formation of a single layer on the sorbent surface considering no secondary interaction of the sorbate. It considers that the sorbent surface contains only one type of binding sites and sorption of one ion per binding site is taking place. The model can be described as

$$q = \frac{\theta q_{\max} C_e}{1 + \theta C_e} \quad (2.3)$$

$q$  : biosorption capacity

$q_{\max}$  : maximum biosorption capacity (complete surface saturation)

$\theta$  : constant related to adsorption energy

$C_e$  : equilibrium concentration of metal ions

The Freundlich model considers no surface saturation and can be expressed as

$$q = k C_e^{1/n} \quad (2.4)$$

where  $k$  and  $n$  are model constants.

Various researchers utilized either or both of these models to describe biosorption phenomena of different sorbent-sorbate systems. Pagnanelli et al. (2000) studied both models for fitting the biosorption data of sorption of Cu and Cd on living biomass *Arthrobacter sp.* and found that the Freundlich isotherm provided a better fit for this system. Annadurai et al. (2003) also found that the Freundlich model fit better than the Langmuir model for biosorption of Cu, Co, Ni, Zn, and Pb on banana and orange peels. Jumle et al. (2002) were also able to fit the sorption of Hg, Pb, and Zn ions using the Freundlich isotherm model.

The Langmuir isotherm provided a better fit than the Freundlich isotherm model in the case of biosorption of Cr by seaweeds (Cossich et al., 2002). Hashim and Chu (2004) were able to fit the biosorption data for Cd onto seaweeds using the Langmuir isotherm. Say et al. (2000) used the Langmuir isotherm to model biosorption of Pb and other metals onto a fungus used as biosorbent. Reddad et al. (2002) also modeled biosorption of Ni and Cu ions on sugar beet pulp using the Langmuir isotherm and obtained a good fit of the data.

Since both of these models are widely used for biosorption and are easily interpretable, we decided to model biosorption of Pb by citrus peels using both the Langmuir and the Freundlich models, due to their simplicity and good predictive ability.

## 2.6 Regeneration of Sorbent

Desorption of metal ions from the sorbent surface after the biosorption process has been extensively studied previously (Annadurai et al., 2003; Aldor et al., 1995; Gloaguen and Morvan, 1997; Harel et al., 1998). The desorption can be carried out by acidification of spent sorbent material using mineral acids such as hydrochloric acid (HCl), sulfuric acid (H<sub>2</sub>SO<sub>4</sub>), or nitric acid (HNO<sub>3</sub>). Usually biosorbents are stable and can be reused several times after recovering metal ions. Biosorbents are usually cheap materials and can be burnt after regeneration. A metal removal and recovery scheme for biosorption can be described as:

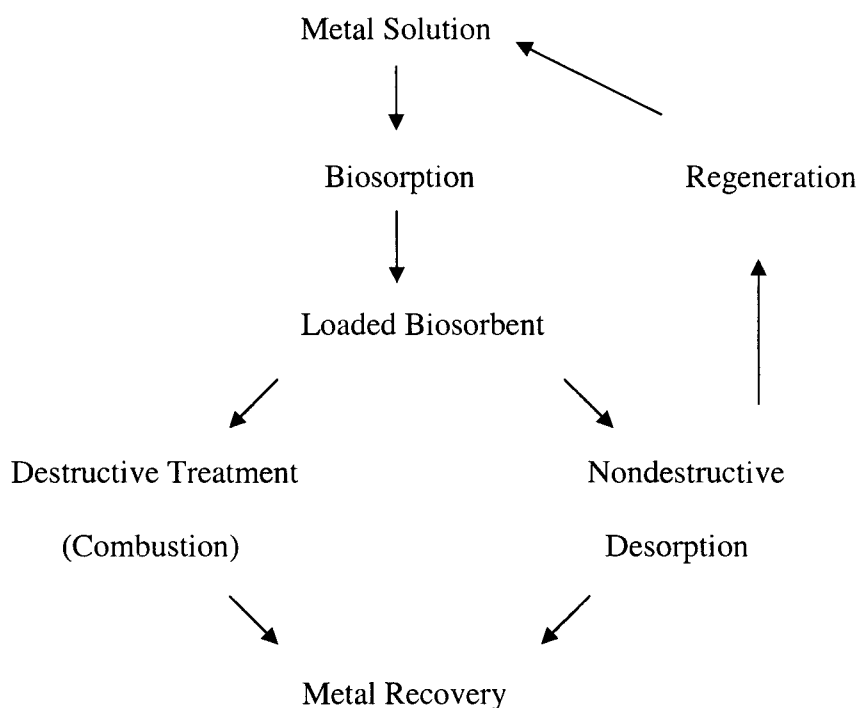


Figure 2.1: Schematic diagram of biosorption process

## Chapter 3

### Materials and Methods

#### 3.1 Material Selection

All experiments were conducted using double de-ionized water and ACS or reagent grade chemicals. Low methoxylated pectin (LM), with methoxy content of 9% and high methoxylated pectin (HM), with methoxy content of 64% were supplied by Sigma-Aldrich. Dried and ground orange peels (CitraSorb™ STD grind: Valencia ORG) as shown in Figure 3.1 were supplied by Biotex Corporation. These peels were sieved into definite sizes and were not washed or protonated in order to maintain their original properties. The nitrate salt of Pb was used, assuming that  $\text{NO}_3^-$  ions do not interfere with the sorption equilibrium. Nitric acid and sodium hydroxide were used for pH adjustment. Sodium nitrate was used for adjusting the ionic strength of the solution.

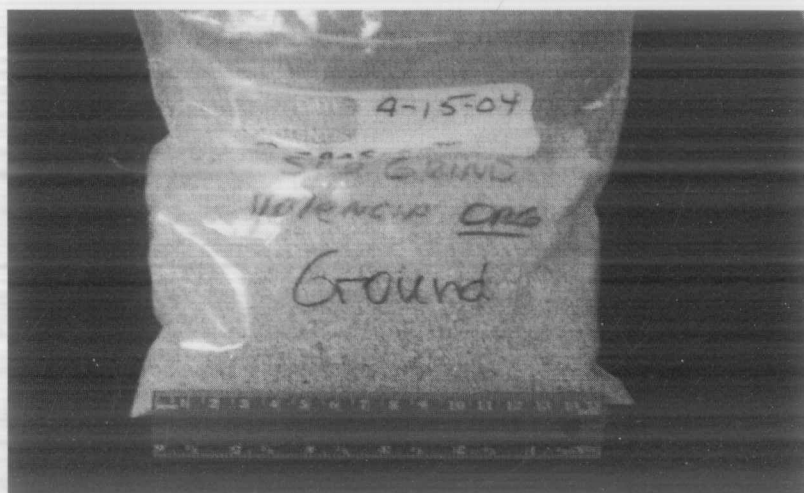


Figure 3.1: Dried and ground orange peels donated by Biotex Corporation

### 3.2 Preliminary Experiments

Preliminary experiments were carried out in order to select proper experimental conditions. The first step was to investigate the formation of pectin gel in the solution by addition of Pb to the solution. Pectin features good gel formation properties in the presence of Ca or Mg. We found that a strong gel formed upon addition of Pb metal ions to the pectin solution in double de-ionized water. The thickness of gel increased with the concentration of Pb.

We decided to conduct our experiments at controlled conditions where direct precipitation could be avoided. These conditions were found by carrying out computer modeling using Visual Minteq. A solubility diagram (Figure 3.2) was prepared for a background electrolyte concentration of 0.01 M NaNO<sub>3</sub>.

This solubility diagram indicates that at pH values of 6 and above, precipitation of PbO is very likely. We also conducted preliminary experiments at pH 8 for different values of Pb, pectin, and background electrolyte concentrations and achieved almost 99% Pb removal, which was likely due to direct precipitation along with biosorption (Balaria et al., 2005). The results of these preliminary experiments are shown in Appendix B. Therefore, in order to avoid direct precipitation we decided to study biosorption of 10<sup>-4</sup> M Pb (maximum allowable concentration) by 0.1 g pectin at a pH 5, with a background electrolyte concentration of 0.01 M NaNO<sub>3</sub>, and at room temperature (21-25 °C). These reaction conditions are indicated by the circular area in the Figure 3.2.

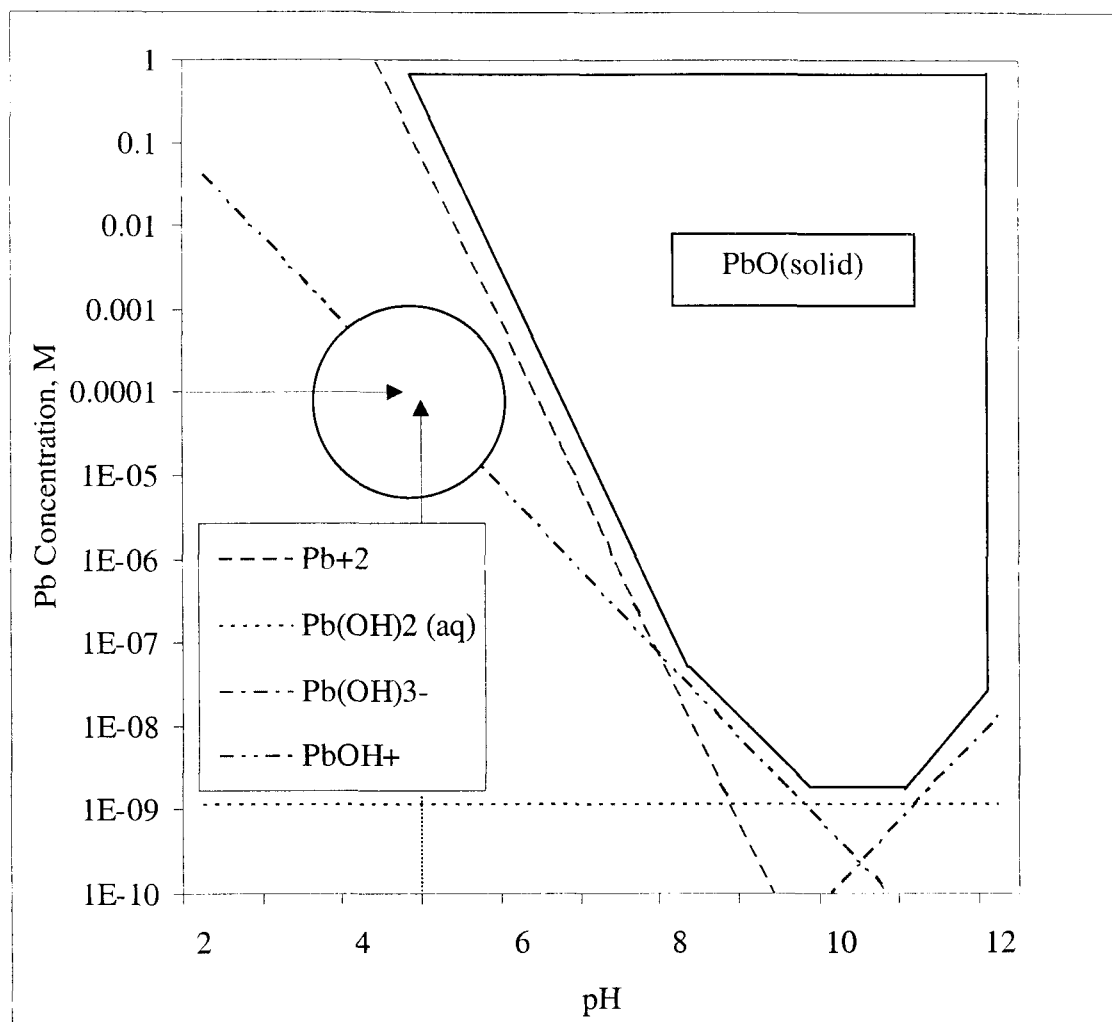


Figure 3.2: Solubility diagram for precipitation of  $Pb(OH)_2$  at 25 °C and a background electrolyte concentration of 0.01 M  $NaNO_3$  (Circle indicates reaction conditions)

### 3.3 Sorbent Characterization

#### 3.3.1 Potentiometric Titrations

Potentiometric titrations were conducted for low methoxylated (LM) and high methoxylated (HM) pectins for two different ionic strength values in order to study the

electrostatic effects on total charge imparted by pectin. These experiments were conducted in closed system conditions ( $N_2$ -atmosphere) in order to avoid any interference and misinterpretations due to dissolved atmospheric  $CO_2$ .

An amount of 0.2 g LM or HM pectin was dissolved in 200 ml double de-ionized water containing 0.01 M and 0.1 M  $NaNO_3$ . Titration experiments were started when the initial pH of the solutions became constant. These pH values were 3.86 for LM pectin and 4.08 for HM pectins irrespective of ionic strength. Known amounts of NaOH were incrementally added and pH values of the solution were measured. These titrations were conducted until a pH value of 10 was obtained for each solution. The added NaOH concentration vs. pH was plotted as a titration curve. Similar experiments were conducted for orange peels for a background electrolyte concentration of 0.01 M  $NaNO_3$ . The surface charge (charge imparted by pectin and peel surfaces) was calculated (as shown below) and plotted as a function of pH.

The electro-neutrality equation of the solution is defined as:

$$[S] + [H^+] + [Na^+] = [OH^-] + [NO_3^-] \quad (3.1)$$

where S is the surface charge in equivalents.  $Na^+$  ions are provided to the solution by  $NaNO_3$  and NaOH. Similarly,  $NO_3^-$  ions are provided by  $NaNO_3$  and  $HNO_3$ . Since  $Na^+$  and  $NO_3^-$  ions provided by  $NaNO_3$  are equal and opposite in charge, their values cancel out in the above equation and only the quantities of  $Na^+$  and  $NO_3^-$  provided by the NaOH

and  $\text{HNO}_3$  need to be considered. Solving Equation 3.1 for S and dividing by sorbent mass yields

$$S \text{ (eq/g)} = [\text{Acid (eq)} - \text{Alkali (eq)} + \text{OH}^- \text{ (eq)} - \text{H}^+ \text{ (eq)}] / \text{mass of sorbent (g)} \quad (3.2)$$

$$S \text{ (C/g)} = S \text{ (eq/g)} \times F \quad (3.3)$$

where Faraday's constant ( $F$ ) = 96485 C/eq

### 3.3.2 FTIR Experiments

Citrus pectins (both LM and HM) and peels were characterized with respect to their surface functional groups using Fourier Transform Infrared Spectroscopy (FTIR). These experiments were conducted using a Thermo Nicolet IR-100 spectrometer. Dry pectins and peels were taken in their original form and mixed with solid KBr at a ratio of 1:100. This mixture was pressed into a film which was used for the experiments. IR absorbance data were obtained for wave-numbers  $400\text{-}4000 \text{ cm}^{-1}$ . IR data were collected, processed, and analyzed using the software Encompass® (Copyright © 2003 by Thermo Electron Corporation).

### 3.4 Binding Evaluation

Binding evaluation experiments were conducted in an open system to simulate practical environmental application. Visual Minteq modeling was performed to confirm that the open system conditions do not lead to precipitation of  $\text{PbCO}_3$  and the  $\text{Pb}(\text{HCO}_3)^+$

concentration is negligible (0.028%) for the given environmental conditions. All experiments were conducted using double de-ionized water and ACS and reagent grade chemicals. Experiments were conducted in acid washed 200 ml Nalgene reactor bottles with continuous stirring using a magnetic stirrer for proper mixing. The general conditions selected for the experiments were: room temperature (21-25 °C), pH 5, background electrolyte concentration of 0.01 M NaNO<sub>3</sub>, Pb concentration 0.1 mM (20.7 ppm), and peels/pectin concentration 0.1 g /L. Samples were filtered using a 0.2- $\mu$ m membrane filter and the Pb concentration of the filtrate was analyzed using Graphite Atomic Absorption spectrometry (Perkin-Elmer AAnalyst 300).

### **3.4.1 Kinetic Experiments**

Kinetic experiments were conducted in order to determine the equilibration time and binding rate for Pb binding by citrus LM/HM pectin or peels. The effect of sorbent size on sorption kinetics was investigated using orange peels with different sizes: smaller than 6 mm, 6 mm to 1 mm, and 1 mm to 3 mm. Sampling times ranged from as low as 2 min to as high as 3 h based on preliminary experiments. 5 ml samples were taken periodically using a syringe and filtered using 0.2- $\mu$ m membrane filters. Data were modeled using both first- and second-order kinetic models.

### **3.4.2 Effect of Environmental Conditions**

Effects of environmental conditions such as pH, co-ion presence, and background electrolyte concentrations were investigated as they can be important factors in governing

overall sorption. All of these experiments were conducted for two different amounts of orange peels: 0.1 g/L and 1 g/L providing limited and excess sites, respectively. A Pb concentration of 0.1 mM was used for all the experiments. Three pH values 3, 4 and 5 were investigated as these can be common in acidic metallic effluents. The industrial effluent streams contain many different metal ions along with lead. We decided to investigate the presence of equimolar divalent metal ions Ca and Ni as they are very common in such waste streams. Background electrolyte concentrations were studied for 0 M,  $10^{-2}$  M, and  $10^{-1}$  M NaNO<sub>3</sub>.

### **3.4.3 Isotherms**

Binding isotherms were prepared by varying the initial metal ion concentration while keeping the sorbent amount fixed. An equilibration time of 3 h was allowed before sampling. The Pb concentration was varied from 20 mg/L to 400 mg/L ( $9.65 \times 10^{-2}$  mM to 1.93 mM). Equilibrium sorption was modeled using the Langmuir and the Freundlich isotherms because of their ease of interpretation.

### **3.4.4 pH Variability Study**

Since all previous experiments were conducted at a constant pH of 5, a pH variability study was conducted to understand how the pH would change due to metal addition. Starting from pH 5, we added 0.1 mM Pb solution repeatedly to a solution containing 0.1 g/L sorbent (LM and HM pectins as well as orange peels). The effects were studied until the pH value became almost constant.

### 3.4.5 Mechanism Investigation

Fourier Transform Infrared Spectroscopy was again used to determine the possible functional groups responsible for binding Pb in the aqueous solution. Solutions containing pectin-Pb gels (initial [Pb]: 0.1 mM) were centrifuged in order to obtain the gel, which was further air dried and used for FTIR analysis. These dried gels were then mixed with KBr at a ratio of 1:100 and compressed into films for FTIR analysis as described in section 3.3.2. Pb loaded peels were filtered out of solution, dried and analyzed in the same manner.

### 3.4.6 Experimental Error Considerations

Some experiments and sampling were chosen at random for duplicate experiments/sampling in order to check reproducibility of results. The relative standard deviations for these samples are tabulated in Appendix C. Since the graphite furnace atomic absorption spectrometer measures concentrations of Pb smaller than 100 ppb, filtrate samples were diluted to bring them into this concentration range and multiplied by the dilution factor to calculate the Pb concentration in the original sample. Three concentration readings were obtained from the spectrometer and analyzed for sample concentration in order to confirm the reproducibility of data. The data points depicted present the concentration values derived from the average of these three concentration readings measured by the instrument, with a relative standard deviation of smaller than 5%.

### 3.4.7 Modeling Error Analysis

In order to check the error in the model fit, the average of sum of squared errors (*SSE*) were calculated for both kinetic and isotherm models. This analysis was performed by taking square of the difference between values of metal removal experimental data ( $q$ ), and those determined by the models ( $q_m$ ) and dividing it by the number of data points ( $p$ ) for each data set.

$$SSE = \frac{\sum^p (q - q_m)^2}{p}$$

SSE values were also used to prepare non-linear models of the Langmuir and Freundlich isotherms. These models were obtained by minimizing the SSE value for the respective model fits and obtaining modified values of model parameters. Such non-linear models were not prepared for kinetic modeling because a very low overall SSE value was obtained with regular linear second-order model, which provided a very good fitting of the experimental data.

## Chapter 4

### Results and Discussion

#### 4.1 Characterization of Sorbents

##### 4.1.1 Sorbent Charge

Potentiometric titrations were conducted in order to estimate overall negative charge equivalents at the conditions of pH and ionic strength employed for kinetic experiments and multivariable analyses. These titrations were conducted at different ionic strengths to evaluate the effect of ionic strength on total charge equivalents. Figures 4.1 and 4.2 represent the titration results for citrus pectins of two different degrees of methoxylation, 9% and 64%, at background electrolyte concentrations of 0.01 M NaNO<sub>3</sub> and 0.1 M NaNO<sub>3</sub>, respectively (S represents the total solution charge imparted by the sorbent material).

These results show that a plateau with stable charge values for a pH range ~ 6 to 9 is attained at 0.8 meq/g for LM pectin and 0.4 meq/g for HM pectin suggesting a significant effect of the methoxylation degree on the net surface charge. However, ionic strength variations over an order of magnitude do not induce any significant impact on the magnitude of charge. These titration curves also suggest that there are functional groups present in the structure of pectin which buffer the solution below pH 5 and above pH 10. These groups may be carboxylic groups ( $pK_a$  3-5) and hydroxyl groups ( $pK_a > 9$ ). Since the pH electrode was calibrated for pH values of 4, 7, and 10, the titration pattern

near pH values of 10 cannot be evaluated quantitatively. Therefore, molecular scale analyses using Fourier Transform Infrared Spectroscopy were performed to investigate the functional groups present in the pectin used.

Figure 4.3 represents total negative surface charge of protonated and original orange peels at room temperature and for a background electrolyte concentration of 0.01 M  $\text{NaNO}_3$ . Protonation was carried out by washing the sorbent material with acid in order to remove metal ions e.g.  $\text{Ca}^{2+}$ , which could be naturally present, bound to the orange peels. Protonation releases these metal ions, replacing them with protons which could be relatively easily released in aqueous solution. Therefore the protonated peels show a higher negative surface charge in Figure 4.3 than the original unprotonated peels.

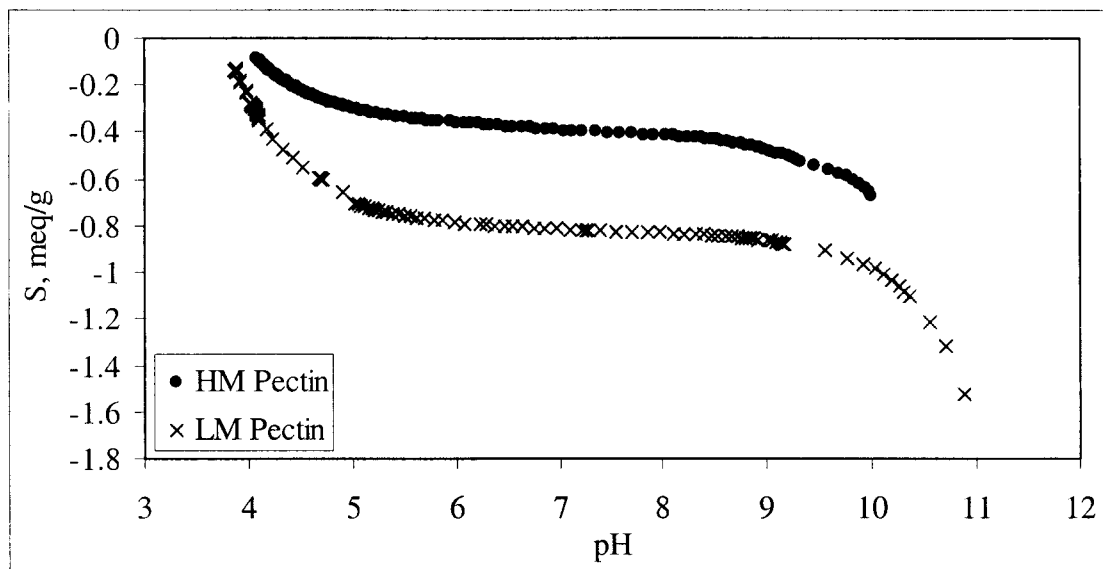


Figure 4.1: Potentiometric titrations of LM and HM pectins at a background electrolyte concentration of 0.01 M  $\text{NaNO}_3$

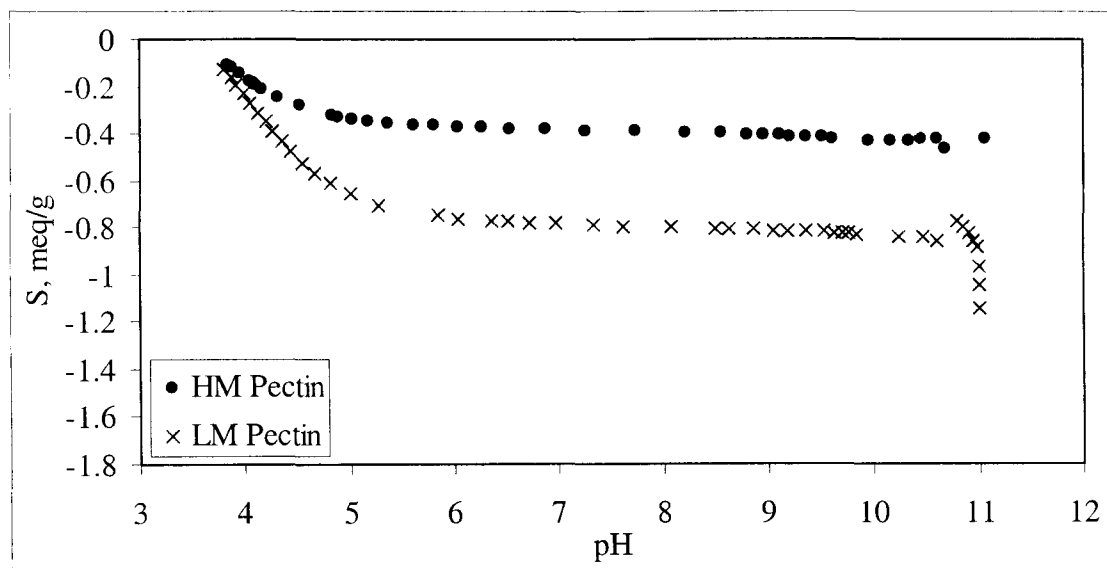


Figure 4.2: Potentiometric titrations of LM and HM pectins at a background electrolyte concentration of 0.1 M  $\text{NaNO}_3$

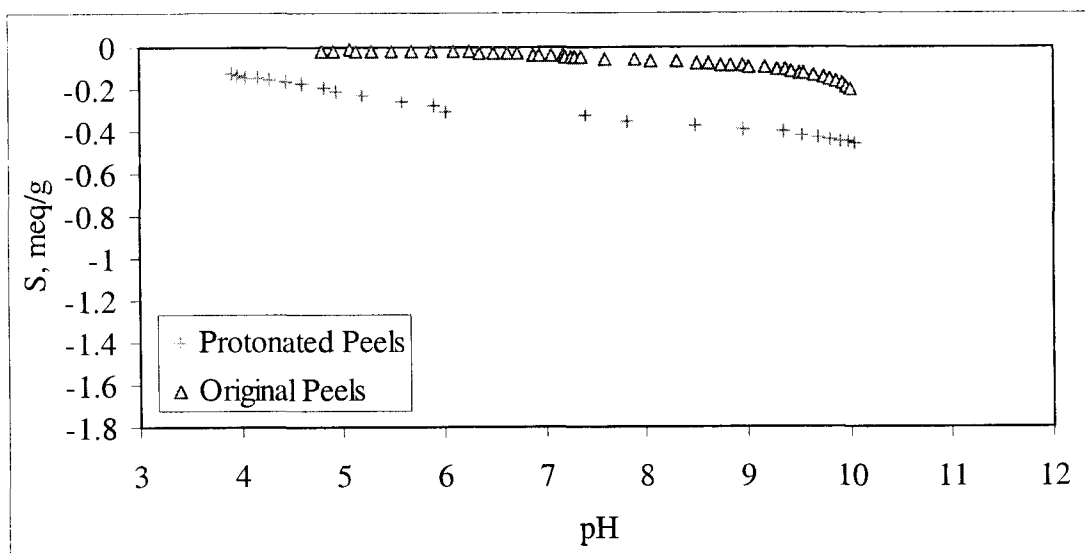


Figure 4.3: Potentiometric titrations orange peels at a background electrolyte concentration of 0.01 M  $\text{NaNO}_3$

The surface charges of citrus pectins and orange peels at pH 5 and background electrolyte concentration of 0.01 M NaNO<sub>3</sub> are presented in Table 4.1. These results suggest that low methoxylated pectin, which contains the highest amount of -COOH groups, contains the most negative charges followed by high methoxylated pectin and then orange peels.

Table 4.1: Total surface charge of sorbents as determined by potentiometric titrations at pH 5 and a background electrolyte concentration of 0.01 M NaNO<sub>3</sub>

Material	Type	Surface charge at pH 5	
		meq/g	C/g
Pectin	LM	-0.702	-67.74
	HM	-0.3	-28.97
Peels	Original	-0.014	-1.313
	Protonated	-0.23	-22.3

#### 4.1.2 Sorbent Functional Groups

Fourier Transform Infrared Spectroscopic results revealed that both the pectins and the peels have very similar spectra, which confirmed that pectin is an important component of orange peels and has similar functional groups (Figure 4.4). All spectra have a hydroxyl (-OH) peak at wave number  $\sim 3500 \text{ cm}^{-1}$ , alkyl (-CH<sub>n</sub>) at wave number

~2920 to 2940  $\text{cm}^{-1}$  peak, ester (-COOR) peak at wave number ~ 1740 to 1750  $\text{cm}^{-1}$ , and carboxylic acid (-COOH) peak at wave number ~ 1625 to 1640  $\text{cm}^{-1}$ . The earlier parts of spectra (i.e. wave numbers 1000 to 1500  $\text{cm}^{-1}$ ) are also quite similar in all the sorbent materials. This part represents various configurations of C, O, N, and H bonds in the pectin and peel structures (Gnanasambandam and Proctor, 1999; Monsoor et al., 2001; Copikova et al., 2001).

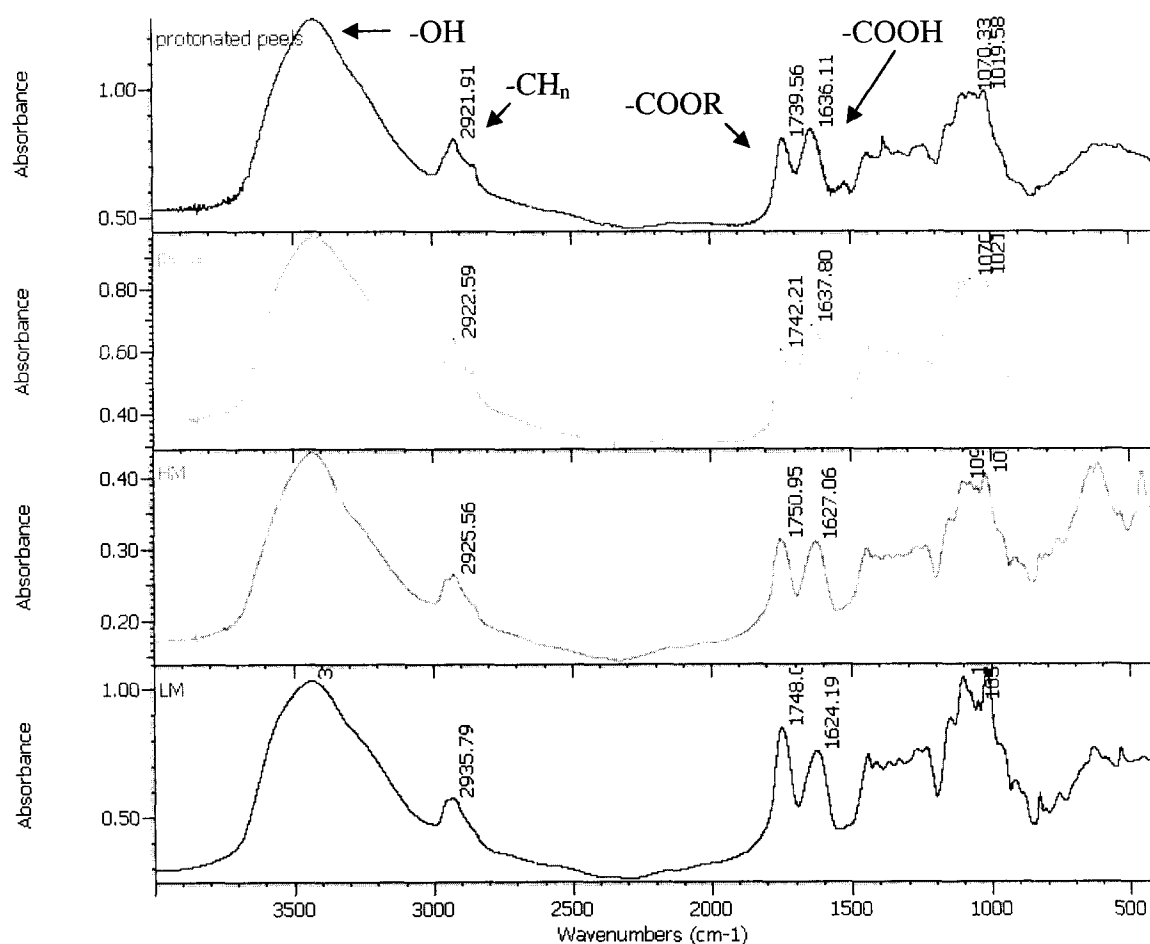


Figure 4.4: FTIR spectra of LM pectin, HM Pectin, orange peels, and protonated orange peels

## 4.2 Biosorption Studies

### 4.2.1 Batch Kinetics:

Kinetic studies are not only necessary to determine the equilibration time for biosorption but also important for designing treatment systems based on the reaction rate. They also provide an indication of the overall biosorption capacity for the sorbent material. We conducted biosorption batch kinetic studies with both low and high methoxylated citrus pectins in order to investigate the effect of methoxylation degree on the rate of biosorption. Since the pectin was in dissolved form prior to the experiment, the Pb binding was related to gelation (gel formation). A gel was observed as soon as the Pb was added to the pectin solution, which suggests immediate binding of Pb by the polymeric chains of pectin.

Figures 4.5 and 4.6 represent the binding of Pb by low methoxylated and high methoxylated pectins. The results suggest that for both low and high methoxylated pectins, around 70% of the total Pb was removed from solution within the first two minutes due to instant gel formation. The gel became denser with time removing increasing quantities of lead from the solution until equilibrium was achieved within 40 minutes at around 85-90 % Pb removal for both types of pectins. From these results we can conclude that both low and high methoxylated pectins have sufficient functional groups to bind the heavy metal ion Pb at the concentrations applied. Since the  $pK_a$  value of  $-COOH$  groups is between pH 3 and 5, they would be predominantly negatively charged, which is favorable for cation uptake. Since the presence of carboxylic groups is

shown by FTIR characterization, we can infer that these groups may be playing a dominant role in Pb biosorption by pectin.

In order to determine the binding rate constant and capacity, we used pseudo first- and second-order kinetic models. These are the most commonly used kinetic models and either of them can provide better fit depending on the biosorbent and metal ions. Ajmal et al. (2000) found that Ni biosorption by orange peels followed first-order kinetics, whereas Reddad et al. (2002) found that Ni and Cu biosorption by pectin rich sugar beet pulp followed second-order kinetics. Figures 4.7, 4.8 and 4.9 represent the linear forms of these models representing the present study. It is clear from Figure 4.7 that the gelation of Pb-pectin does not follow first-order kinetics as the linear fitting value of  $R^2$  is 0.57 and 0.37 for LM pectin and HM pectins, respectively. Moreover, the value of  $q_e$  for Equation 2.1 had to be assumed as the maximum value of the experimental data, which causes further uncertainty in data modeling. The  $R^2$  values for the second-order kinetic model were 1 and 0.9999 for LM and HM pectins, respectively, suggesting a very good fit (Figures 4.8 and 4.9). The fitting of data using this model is shown in Figures 4.5 and 4.6 and the parameters are tabulated in Table 4.2. The fact that the second-order model describes the kinetics of Pb biosorption by orange peels and citrus pectin confirms that monovalent negatively charged functional groups are responsible for binding. Pb is a divalent ion and if it binds with two monovalent negatively charged surface sites in order to balance the reaction stoichiometry, the rate will be proportional to the square of the remaining surface sites, which is the assumption for a second-order reaction.

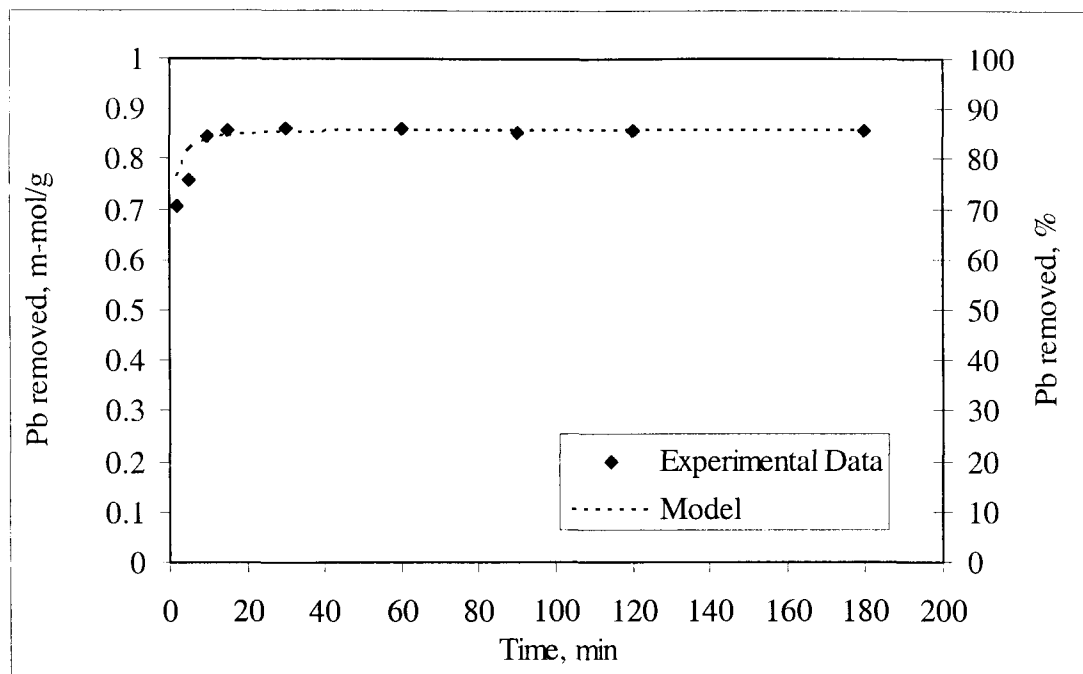


Figure 4.5: Pb-LM pectin kinetic data modeling using a pseudo second-order model

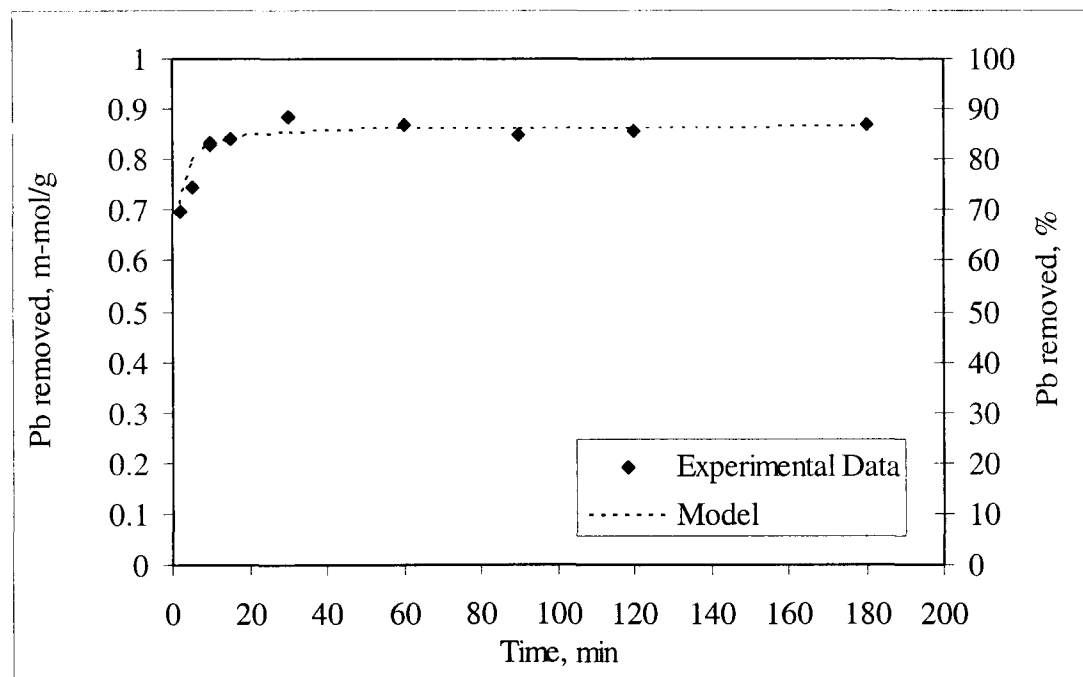


Figure 4.5: Pb-HM pectin kinetic data modeling using a pseudo second-order model

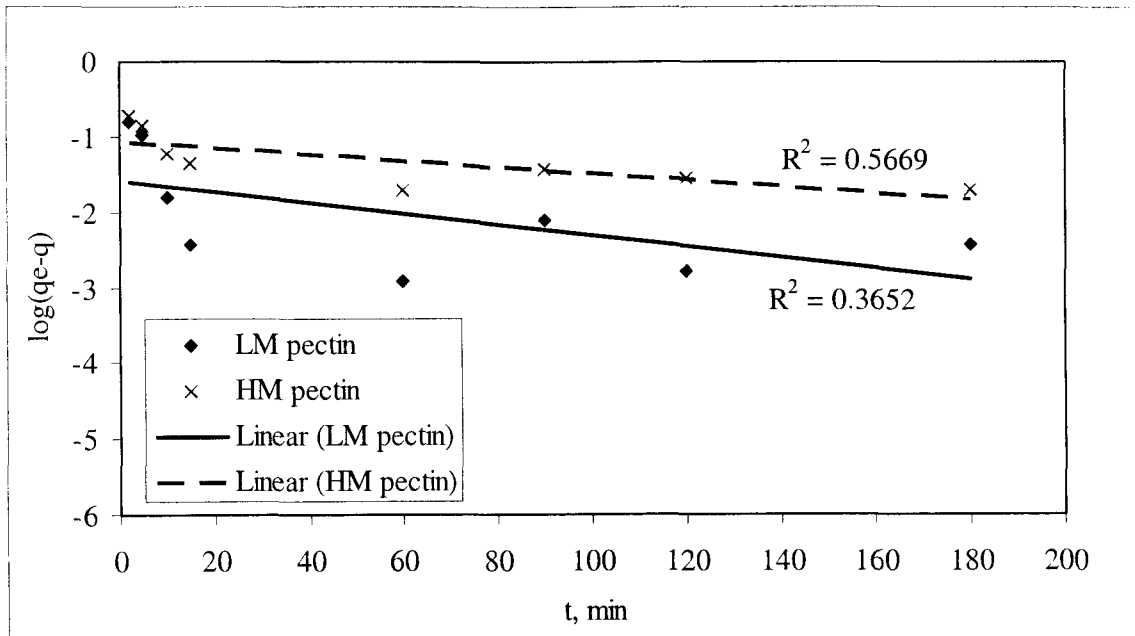


Figure 4.7: Linear fitting of Pb-pectin kinetic data using a pseudo first-order model

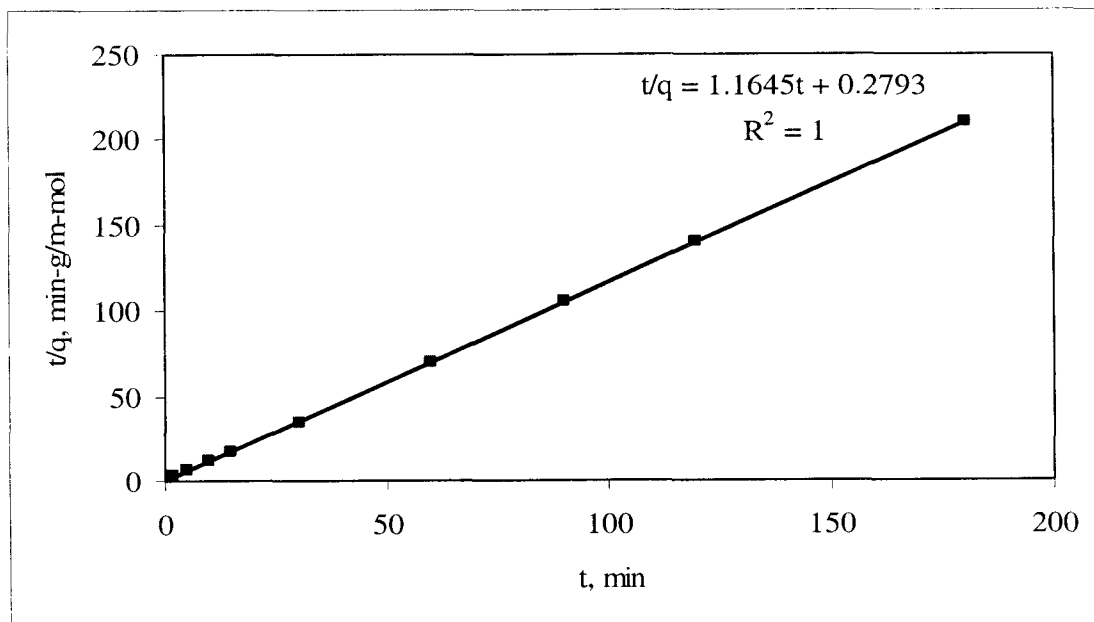


Figure 4.8: Linear fitting of Pb-LM pectin kinetic data using a pseudo second-order model

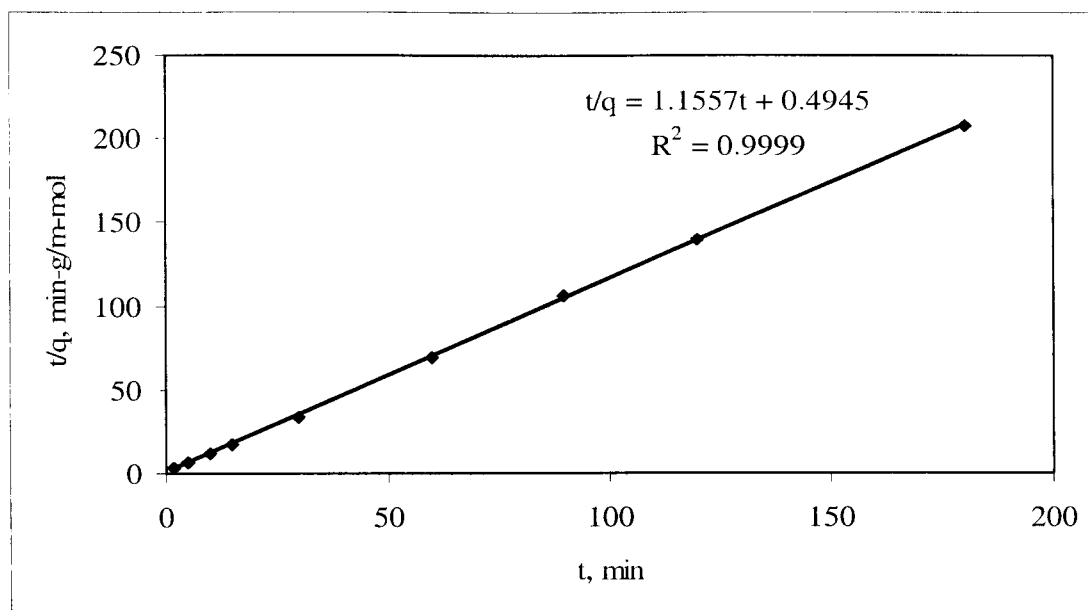


Figure 4.9: Linear fitting of Pb-HM pectin kinetic data using a pseudo second-order model

Table 4.2: Second-order kinetic parameters for Pb gelation with pectin

Sorbent	k, g/mmol-min	q, mol/g	R <sup>2</sup>	SSE
LM Pectin	2.64	0.86	1	7.87E-04
HM Pectin	2.02	0.87	0.9999	5.27E-04

Figures 4.10, 4.11, and 4.12 present binding of Pb by orange peels of three different sizes: smaller than 6 mm, 6 mm to 1 mm, and 1 mm to 3 mm. As is evident from the graphs, the peels with sizes smaller than 6 mm reached equilibrium within the

first 45 minutes whereas the larger sizes took about two hours to attain equilibrium. Equilibrium metal removal was 80-90 % for smaller sizes and 70-80% for larger sizes (1.0 to 3.0 mm).

Comparison of pseudo first-order and second-order models for fitting the data of Pb sorption by all the three sizes of peels showed that the pseudo second-order model provided a better fit for all the three sizes of peels (Figures 4.13 to 4.16). The  $R^2$  values were greater than 0.99 for all the three peels for the pseudo second-order model, whereas those for the pseudo first-order model were  $<0.8$  in all cases.

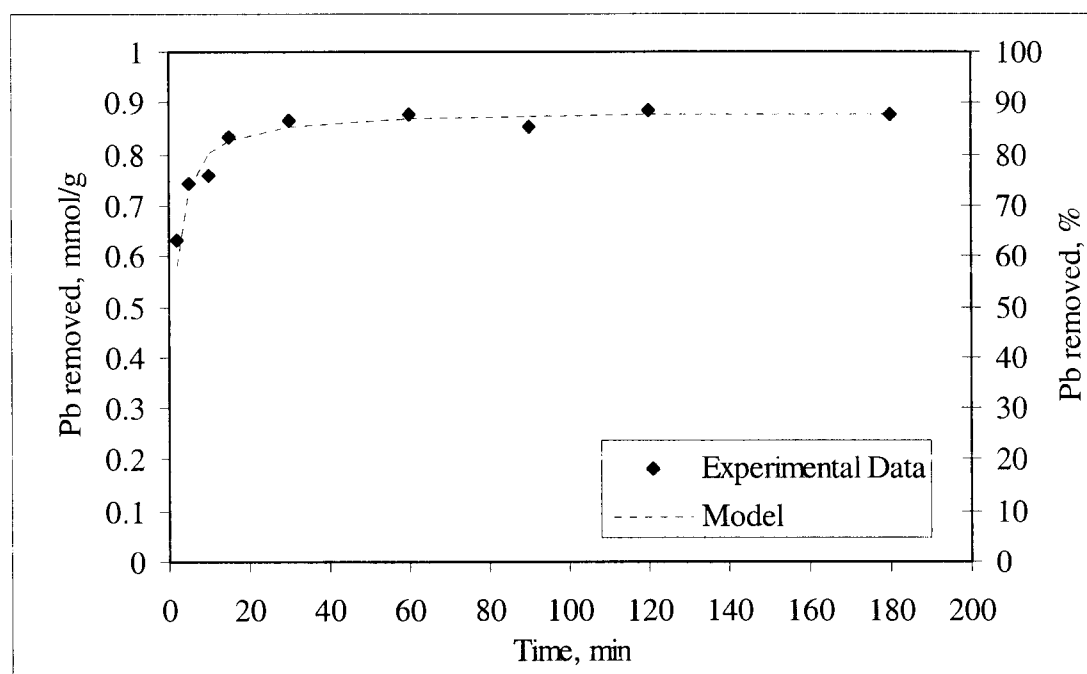


Figure 4.10: Pb-peels (< 0.6 mm) kinetics modeling using a pseudo second-order model

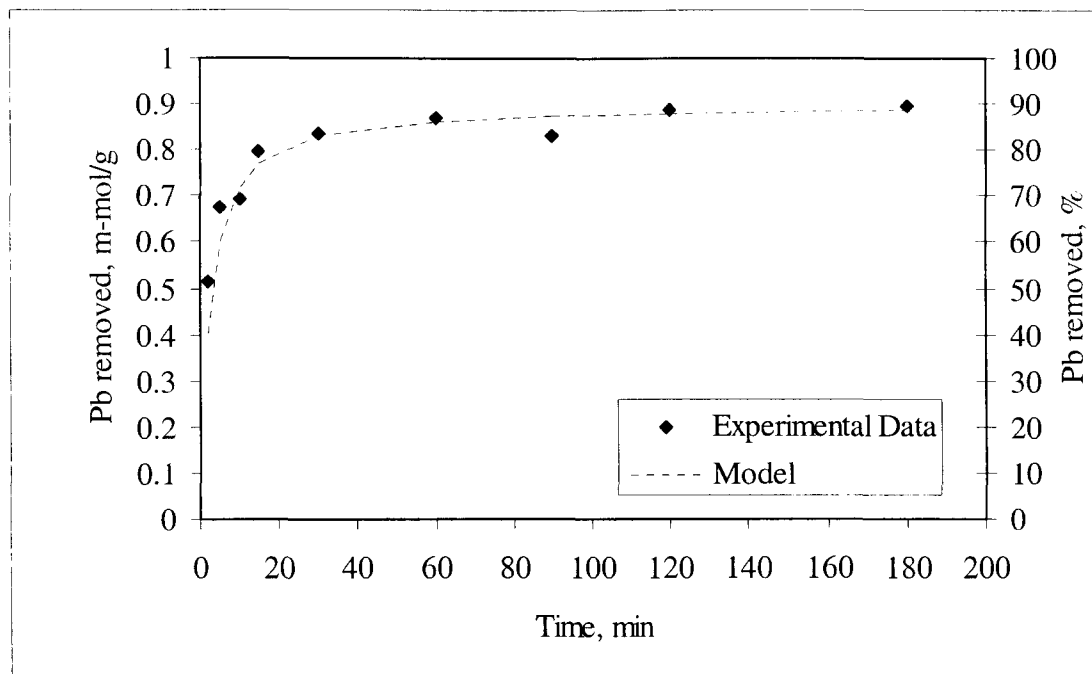


Figure 4.11: Pb-peels (0.6-1.0 mm) kinetics modeling using a pseudo second-order model

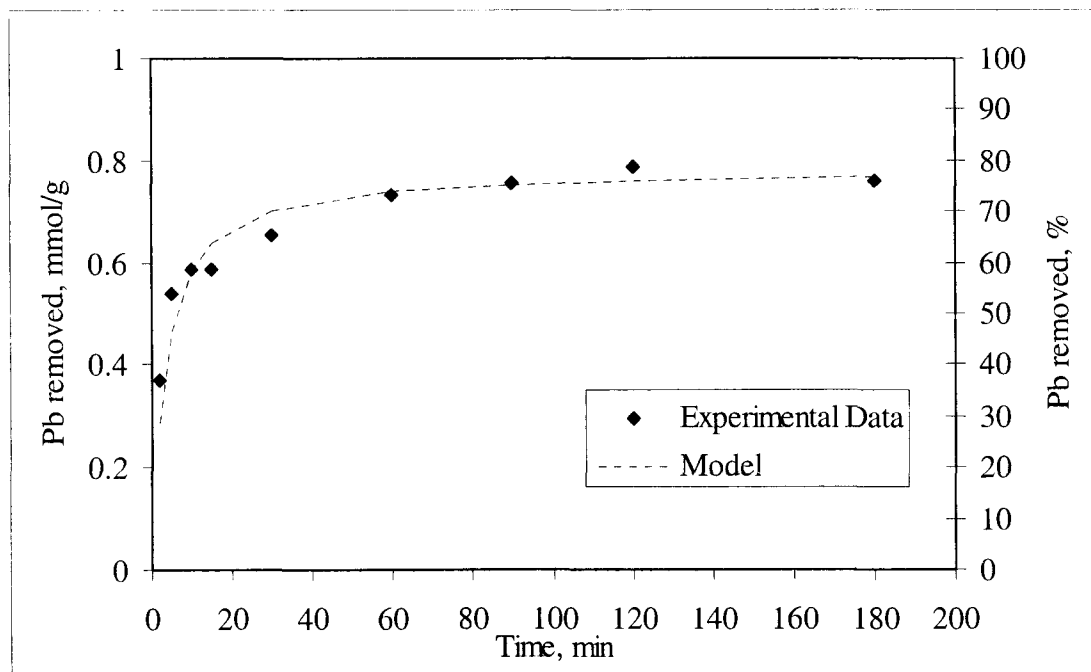


Figure 4.12: Pb-peels (1.0-3.0 mm) kinetics modeling using a pseudo second-order model

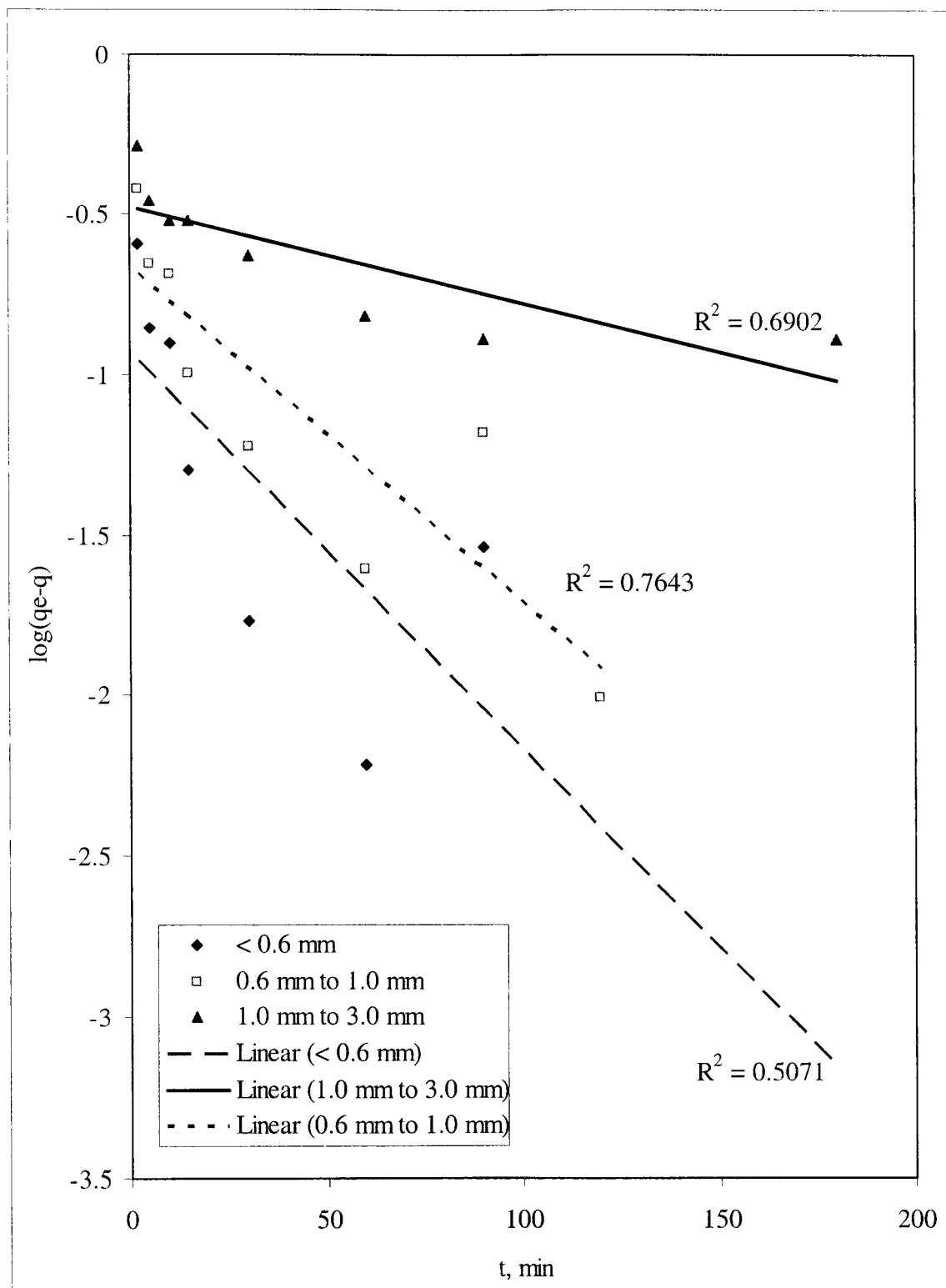


Figure 4.13: Pb-peels kinetic data fitting using a linearized pseudo first-order model

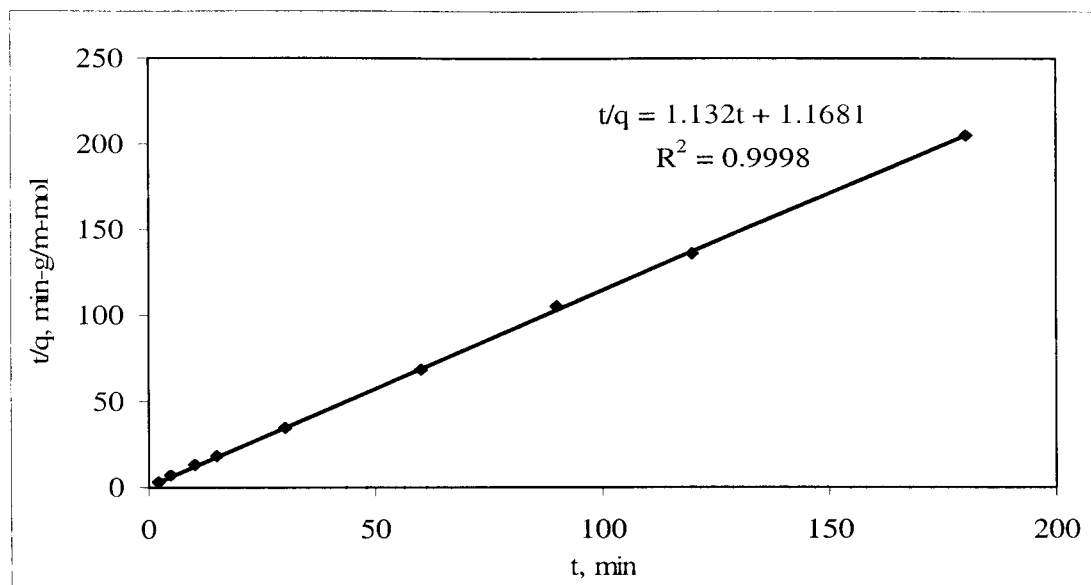


Figure 4.14: Pb-peels (<0.6 mm) kinetic data fitting using a linearized pseudo second-order model

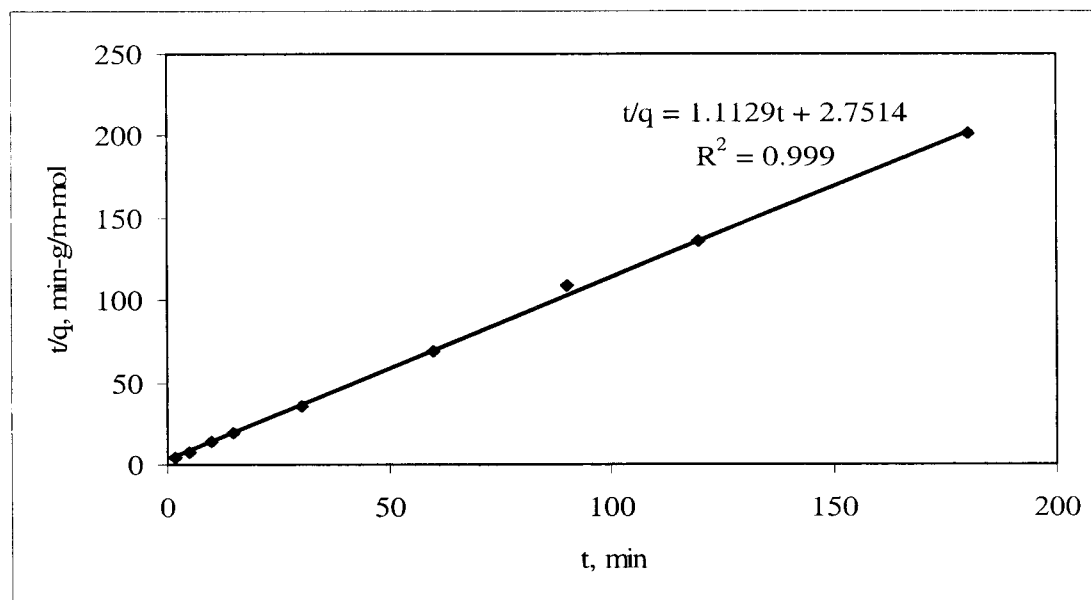


Figure 4.15: Pb-peels (0.6-1.0 mm) kinetic data fitting using a linearized pseudo second-order model

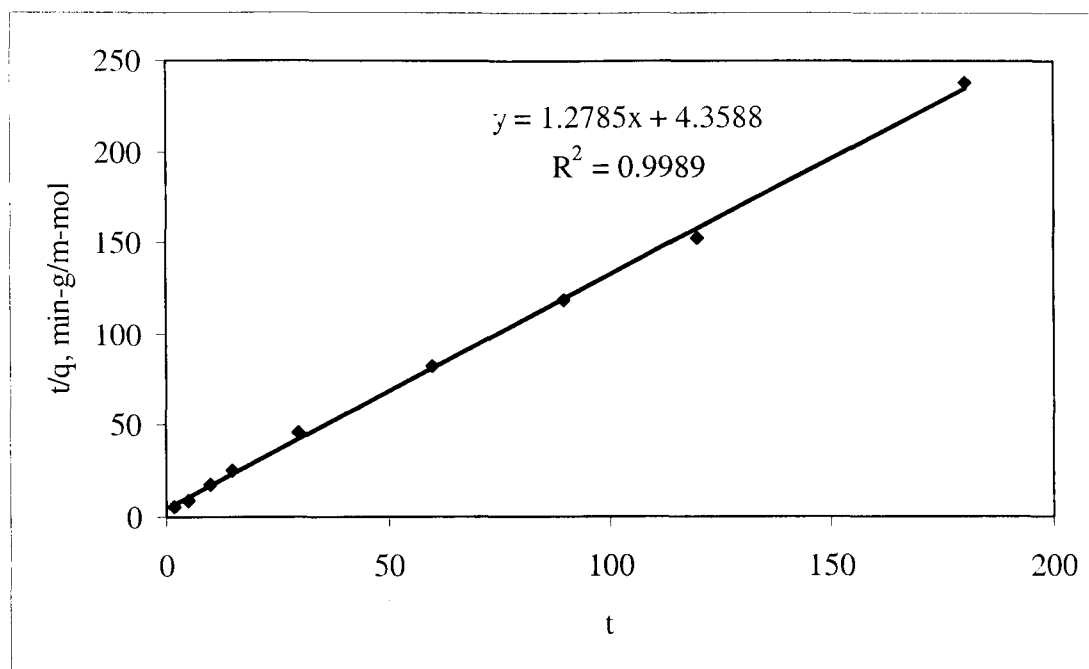


Figure 4.16: Pb-peels (1.0-3.0 mm) kinetic data fitting using a linearized pseudo second-order model

Table 4.3 summarizes the values of rate constants ( $k$ ) and equilibrium capacities ( $q$ ) for the three sizes of peels. Both rate constant and capacity were found to be dependent on the size, being higher for smaller sizes. The peels smaller than 0.6 mm have a rate constant of 0.67 g/mmol-min, which is significantly higher than that of peels for larger sizes (0.29 for 0.6 to 1.0 mm and 0.14 for 1.0 to 3.0 mm). The binding capacity for the two smaller sizes is almost equal,  $\sim 0.9$  mmol/g, and slightly higher than that for the peels of size 1.0 to 3.0 mm ( $\sim 0.8$  mmol/g). These results indicate that the sorption rate is affected by mass transfer, since peels of smaller sizes allowed faster sorption. The fact that the equilibrium sorption capacities of all three materials were similar indicates that

this sorption is not only a surface phenomenon but that Pb is able to penetrate into the peel particles. The sorption capacity of small particles was only slightly higher in spite of much larger external surface area. Since it is less practical to use the very small size (which is  $<0.6$  mm), we used the size 0.6-1.0 mm and allowed an equilibration time of 3 hours for all further experiments.

Furthermore, the binding capacity was found to be higher than the one calculated using potentiometric titration for both types of citrus pectin and the orange peels. This result can in part be attributed to the fact that Pb ions were forcing the functional groups to release protons and bind themselves. A pH variability study was conducted to confirm this phenomenon and it is presented in Section 4.2.4.

Table 4.3: Second-order kinetic parameters for Pb biosorption by orange peels

Size	k, g/mmol-min	q, mmol/g	R <sup>2</sup>	SSE
< 0.6 mm	0.67	0.88	0.9998	5.50E-04
0.6-1.0 mm	0.29	0.90	0.999	2.47E-03
1.0-3.0 mm	0.14	0.78	0.9989	1.93E-03

#### 4.2.2 Effect of Environmental Conditions

After studying the biosorption kinetics of orange peels and investigating the effect of methoxylation degree and sorbent size, we decided to study the effects of different environmental conditions on Pb uptake by orange peels. These conditions include pH, ionic strength, and the presence of equimolar concentrations of co-ions Ca and Ni. We conducted these analyses for two different amounts of sorbent materials which were 1 g/L and 0.1 g/L at a Pb concentration of 0.1 mM. Two different amounts of orange peels were studied in order to investigate the effect of these environmental variables in cases of with limited and excess amounts of surface binding sites.

Figures 4.17 and 4.18 represent the effect of pH on biosorption by 0.1 g/L and 1 g/L orange peels, respectively. The results show that a decrease in pH leads to a decreased removal of Pb from the aqueous solution. This pattern was observed for both excess and limited surface sites. The pattern is analogous to the results of Annadurai et al. (2003), who found an increase in metal ion uptake by banana and orange peels with an increase in pH of the solution. The results can be attributed to the fact that at the higher pH values, the higher degree of dissociation of the surface functional groups leads to more available negative surface sites and higher metal uptake. The results also show that when enough sorbent is available, effective removal of over 90% can be achieved even at lower pH values.

The effects of competing ions on Pb removal by orange peels can be observed in Figures 4.19 and 4.20. Figure 4.19 shows that in the case of limited surface sites, Ca ions are very weak competitors compared to Pb and do not interfere with its biosorption, whereas the Ni ions decrease the overall removal of lead by competing with Pb. However, when the surface sites are in excess (Figure 4.20), neither of the ions interfere much with Pb for sorption and overall removal is affected only by about 2 %. The results confirm findings of Hashim and Chu (2004), who found that for Cd sorption by *Sargassum* biomass, the sorption of Cd decreases with presence of co-existing Ca ions.

Figures 4.21 and 4.22 show the effect of ionic strength on the adsorption of Pb ions on orange peels. In case of excess sites, an increase in ionic strength slightly decreases the sorption. These results are consistent with study of Lee et al. (1999), who found a slight decrease in metal uptake by apple waste with ionic strength increase. The decreased removal at higher ionic strength can be attributed to competition of metal ions with  $\text{Na}^+$  ions in order to balance the negative surface charge. However, when the surface sites are limited, increased ionic strength increased the overall removal. A theoretical metal speciation study for a solution with 0.1 mM Pb in an open system revealed that if no  $\text{NaNO}_3$  was added, virtually all Pb was present as  $\text{Pb}^{2+}$ , and at 0.01 M  $\text{NaNO}_3$  still over 90 % of Pb occurred as  $\text{Pb}^{2+}$ . However at 0.1 M  $\text{NaNO}_3$  only 62 % occurs as  $\text{Pb}^{2+}$  while 34 % occurs as  $\text{PbNO}_3^+$ . This change in speciation must be responsible for increased binding at these conditions. It is possible that total Pb binding increases because each  $\text{PbNO}_3^+$  ion only requires one binding site compared to two sites per  $\text{Pb}^{2+}$ .

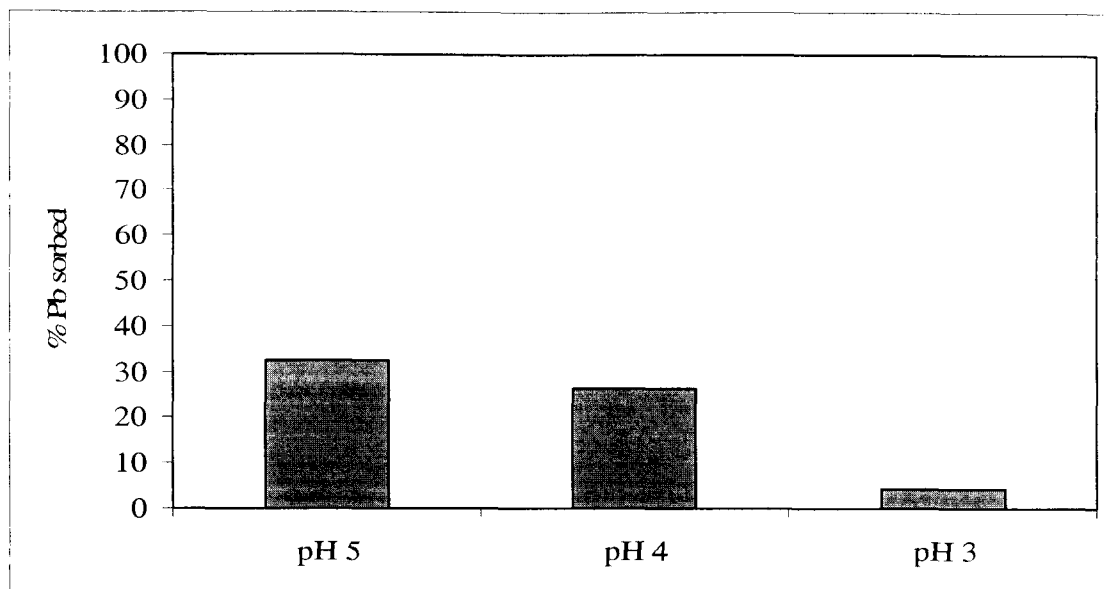


Figure 4.17: Effect of pH on biosorption of 0.1 mM Pb by 0.1 g/L peels at room temperature

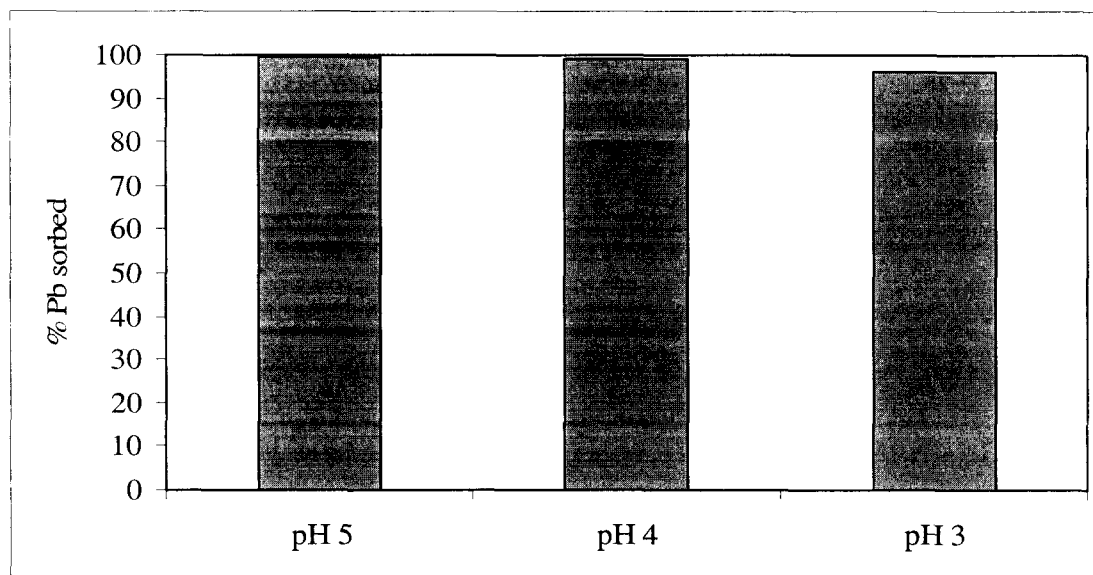


Figure 4.18: Effect of pH on biosorption of 0.1 mM Pb by 1 g/L peels at room temperature

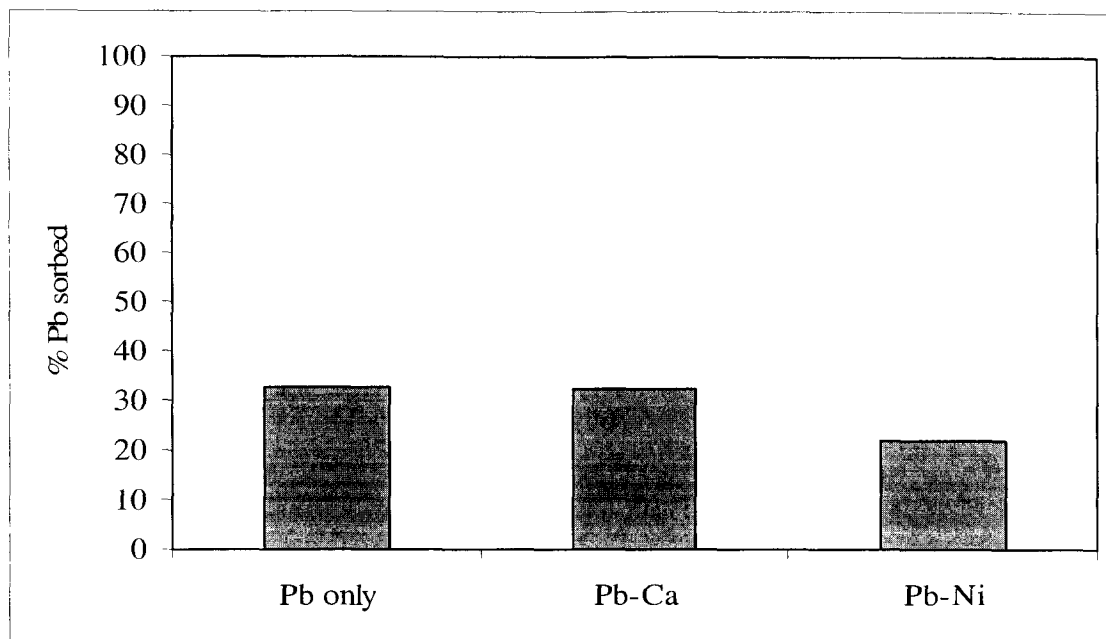


Figure 4.19: Effect of co-ions on biosorption of 0.1 mM Pb by 0.1 g/L peels at room temperature and pH 5

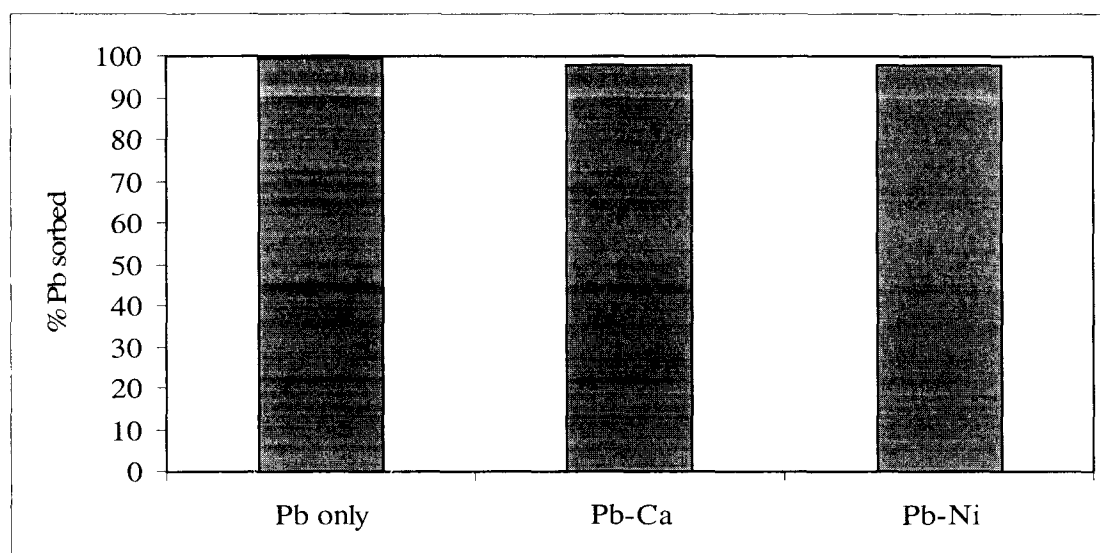


Figure 4.20: Effect of co-ions on biosorption of 0.1 mM Pb by 1 g/L peels at room temperature and pH 5

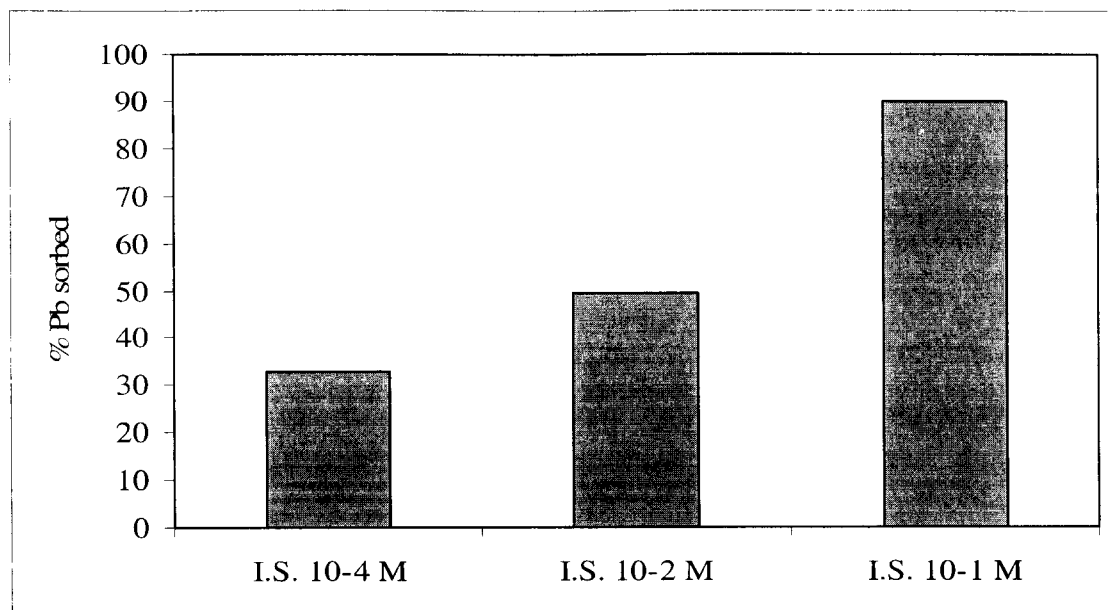


Figure 4.21: Effect of ionic strength (NaNO<sub>3</sub> as background electrolyte) on biosorption of 0.1 mM Pb by 0.1 g/L peels at room temperature and pH 5

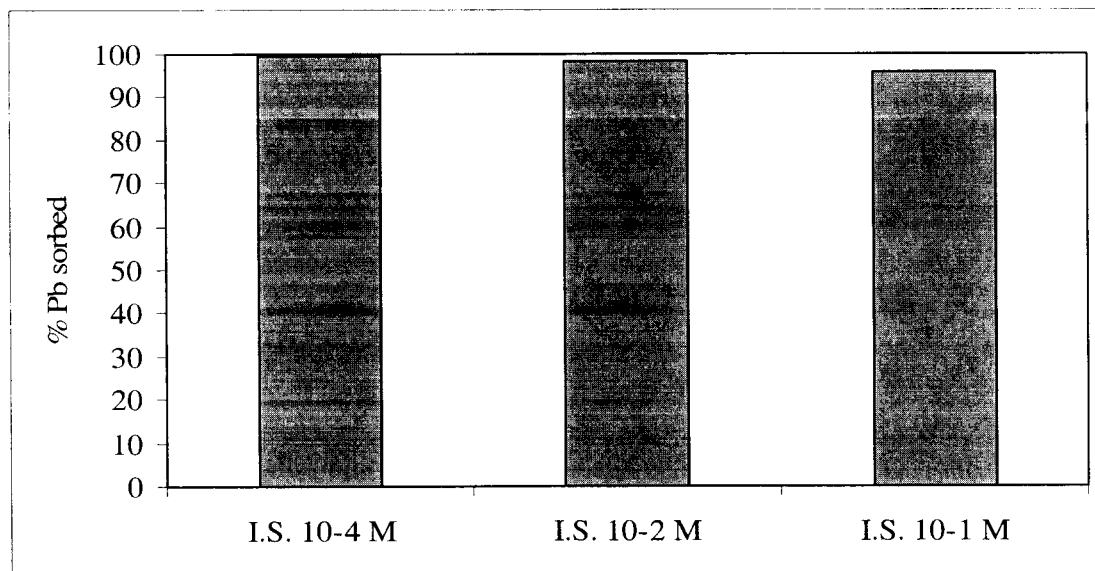


Figure 4.22: Effect of ionic strength (NaNO<sub>3</sub> as background electrolyte) on biosorption of 0.1 mM Pb by 1 g/L peels at room temperature and pH 5

### 4.2.3 Biosorption Isotherm

After investigating biosorption kinetics and the effect of different environmental conditions on Pb uptake, isotherm studies were performed in order to obtain quantitative information about the effect of metal concentration on uptake. For this purpose we studied removal of Pb ions after equilibrium was achieved for different metal concentrations. The resulting Pb uptake as a function of the equilibrium concentration of Pb is presented in Figure 4.23. The data show increased uptake with increasing concentration whereas the slope of the curve gradually decreased. The most common biosorption models representing this phenomenon are the Langmuir and Freundlich models.

The Langmuir model considers formation of a monolayer on the surface with no secondary interactions of sorbates. It can be represented by the equation

$$q_e = \frac{\theta q_{\max} C_e}{(1 + \theta C_e)} \quad (4.5)$$

Where,  $\theta$  (L/meq): Equilibrium adsorption constant

$q_{\max}$  (meq/g): Maximum amount of metal ions per unit mass of biosorbent for saturation of all binding sites.

The Langmuir parameters can be determined from a linearized form of Equation 4.5, written as:

$$\frac{C_e}{q_e} = \frac{1}{\theta q_{\max}} + \frac{C_e}{q_{\max}} \quad (4.6)$$

By plotting  $C_e/q_e$  vs.  $C_e$ , we can obtain the values of constants  $\theta$  and  $q_{\max}$  from the values of slope and intercept (Figure 4.24).

The Freundlich isotherm assumes no surface saturation and can be represented as:

$$q_e = k_f C_e^{1/\eta} \quad (4.7)$$

where  $k_f$  and  $\eta$  are the Freundlich constants which are related to the adsorption capacity of the biosorbent and the adsorption intensity.

The Freundlich parameters can be determined from a linearized form of Equation 4.7 written as:

$$\log q_e = \log k_f + 1/\eta \log C_e \quad (4.8)$$

By plotting  $\log q_e$  vs.  $\log C_e$ , the values of Freundlich constants can be determined from the slope and intercept (Figure 4.25).

After obtaining the Langmuir and Freundlich parameters, the experimental data was modeled and SSE values were calculated for both of these types of isotherms. A non-linear fitting of these models was done by changing the values of these model parameters in order to minimize overall SSE, which provided better fitting of the experimental data.

This fitting is referred as non-linear fitting of these models and is presented in Figure 4.23. The values of model parameters are tabulated in Table 4.4. Even though these non-linear models require more computational efforts to determine the model parameters, they should still be used for data prediction because they provide better fit.

The sorption capacity for Pb biosorption by orange peels was 3.18 mmol/g. Pandey and Thakkar (2004) studied binding capacity of Pb by ion exchange resin containing nitrosocatechol at pH 6 and found the binding capacity to be equal to 0.06 mmol/g. Sorption of Pb by ion exchange resin containing ether linkages was studied by Yang et al. (2004) and they found the sorption capacity to be 2.3 mmol/g at pH 4. These results indicate that biosorption of Pb by orange peels is higher than that by some kinds of ion exchange resins and the first hypothesis holds good. The biosorption capacity calculated by binding isotherms is higher than that predicted by potentiometric titrations, indicating that ion exchange is not the only governing mechanism in this biosorption phenomenon and Pb ions might be replacing protons as well as Ca or other naturally present ions in the original orange peels.

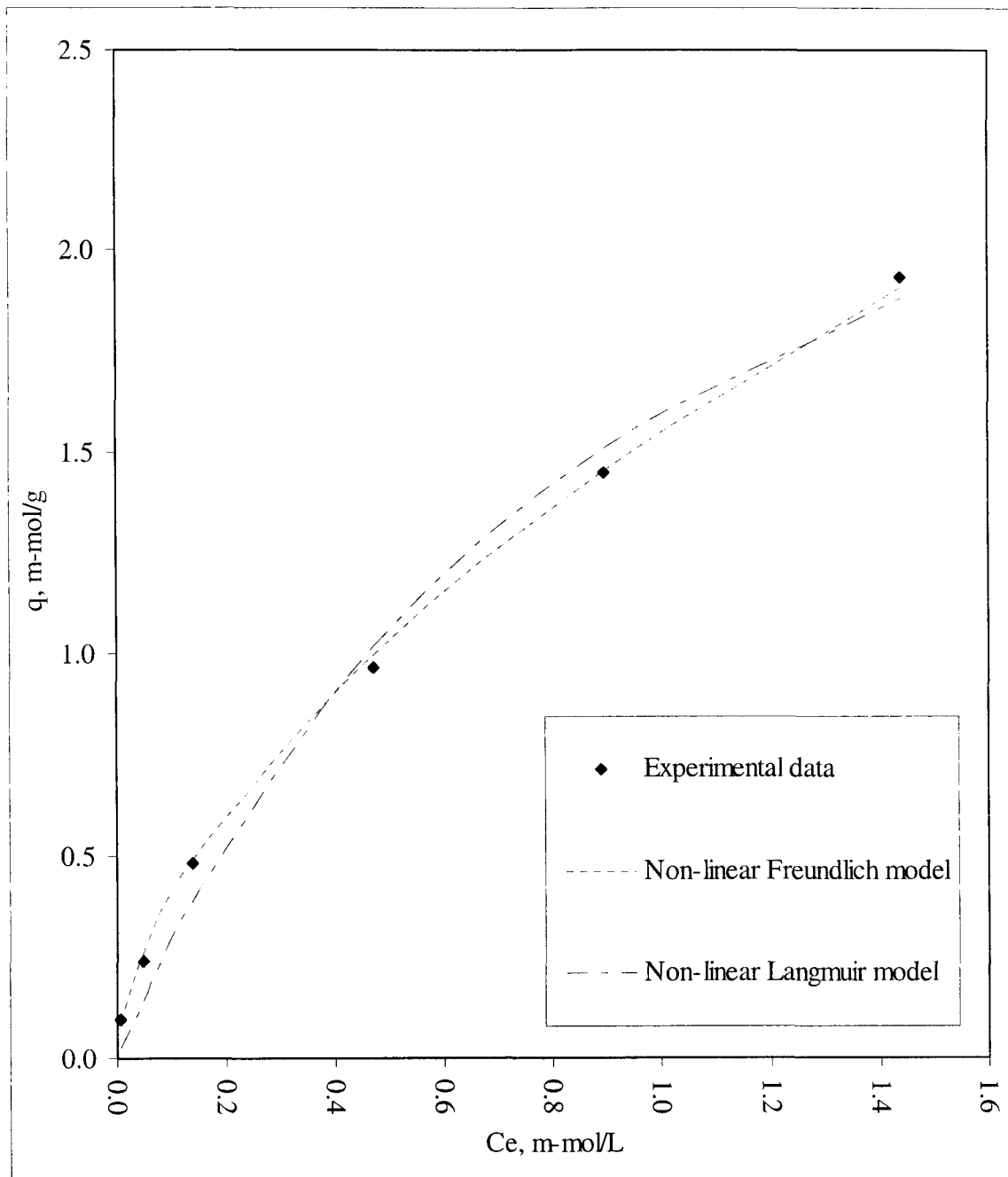


Figure 4.23: Biosorption isotherm modeling for Pb binding by orange peels (size 0.6 mm to 1.0 mm) at room temperature and pH 5

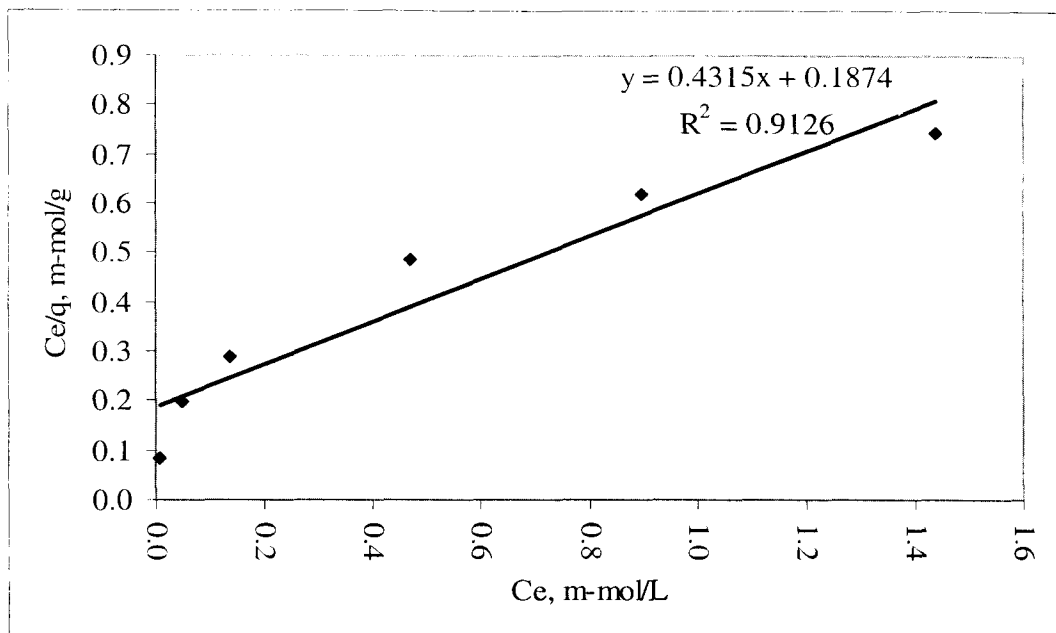


Figure 4.24: Pb-peels isotherm data fitting using a linearized Langmuir model

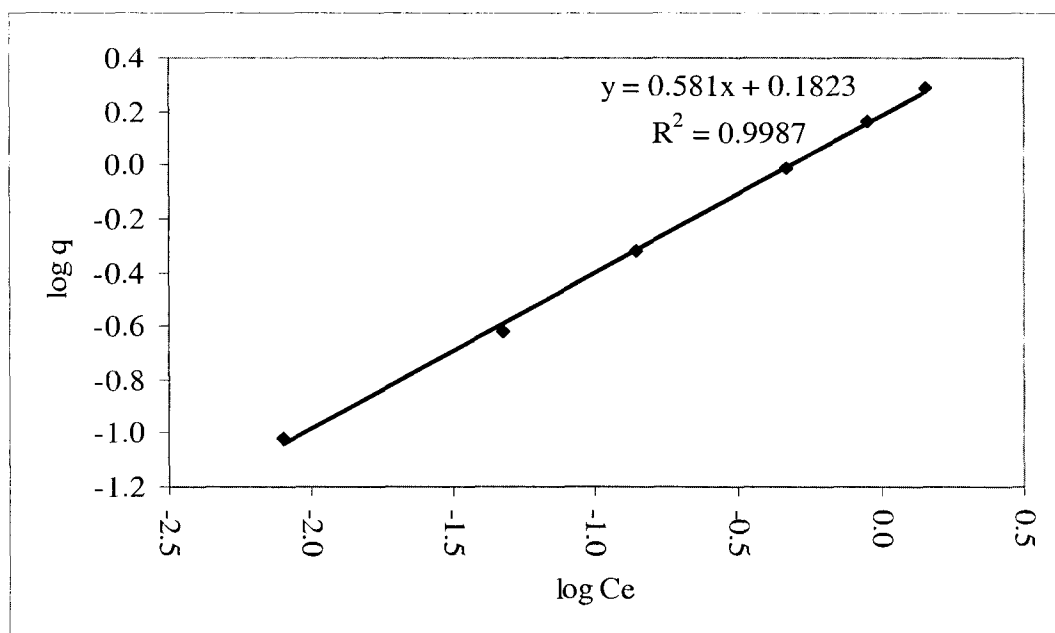


Figure 4.25: Pb-peels isotherm data fitting using a linearized Freundlich model

Table 4.4: Equilibrium parameters for Langmuir and Freundlich isotherm models

Isotherm Model	Model Type	Model Parameters		$R^2$	SSE
Langmuir Isotherm	Linear	$\theta$ = 12.37 L/mmol	$q_{\max}$ = 2.32 mmol/g	0.9126	4.85E-01
	Non-linear	$\theta$ = 1.00 L/mmol	$q_{\max}$ = 3.18 mmol/g	---	5.40E-03
Freundlich Isotherm	Linear	$k_f = 1.20$	$\eta = 1.72$	0.9987	5.87E-02
	Non-linear	$k_f = 1.54$	$\eta = 1.72$	---	3.34E-04

#### 4.2.4 pH Variability Study

Once the rate, capacity, and their dependence on environmental conditions had been investigated for Pb biosorption by orange peels, we decided to learn more about the solution chemistry. Accordingly, we conducted a pH variability study which involved measurement of the pH after addition of a known amount of the sorbate. A 0.1 g/L suspension of peels was used and 0.1 mM Pb solution was added incrementally. The results are described in Figure 4.26 for LM pectin, HM pectin, and orange peels of 0.6 to 1.0 mm size.

From Figure 4.26, we can infer that addition of Pb metal ions causes a decrease in pH of the solution. This decrease in pH can be explained by the replacement of protons from surface functional groups by the divalent Pb ions. This phenomenon is occurring for all the sorbents under consideration: LM pectin, HM pectin, and orange peels. The cumulative values of released protons on incremental addition of Pb are shown in Figure 4.27. This proton release is highest for low methoxylated pectin which contains the highest amount of carboxylic groups (degree of methoxylation ~ 9%). Orange peels show the highest initial rate of such pH decrease but the lowest overall equilibrium decrease of pH. This could be due to easily accessible carboxylic groups on the peels' surface in conjunction with the lowest overall amount of functional groups. This lowest amount of functional groups was also evident in the potentiometric titration study, which shows lowest surface charge for orange peels among the sorbents under investigation.

This study proves the presence of acidic functional groups which undergo acid base reactions at pH 4 to 5 in both citrus peels and pectin and their importance for biosorption. Furthermore, the number of equivalents of protons released on addition of Pb is low compared to the metal uptake under these conditions. This result suggests that at pH 4 to 5 most of the carboxylic acids are in dissociated form and thus ion exchange does not govern the biosorption mechanism.

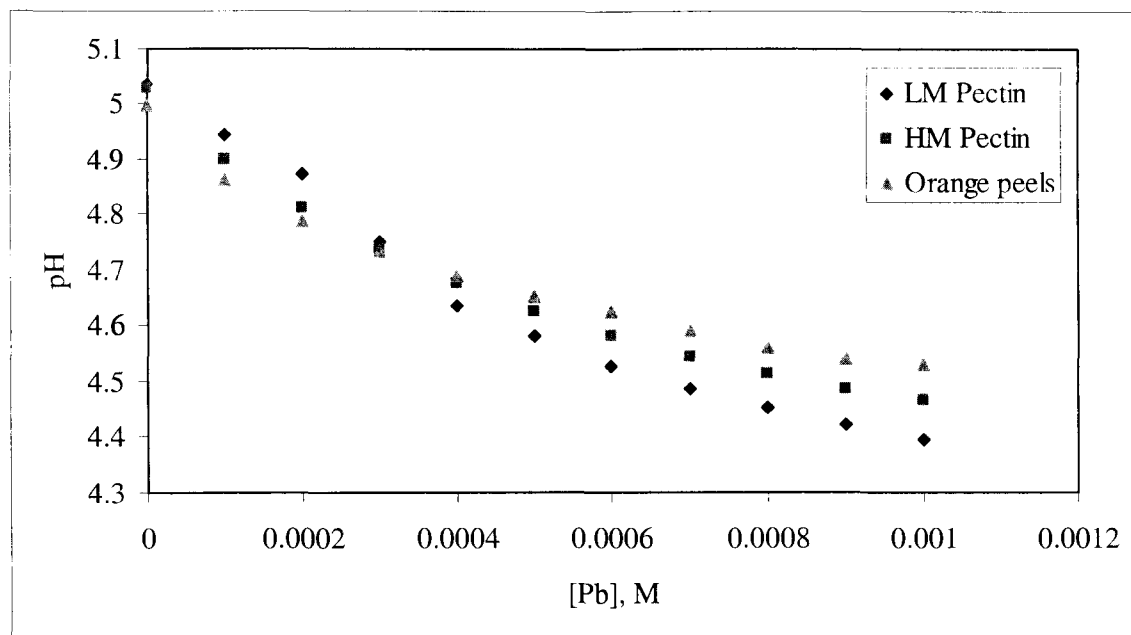


Figure 4.26: pH variability study for Pb sorption by citrus pectin and peels

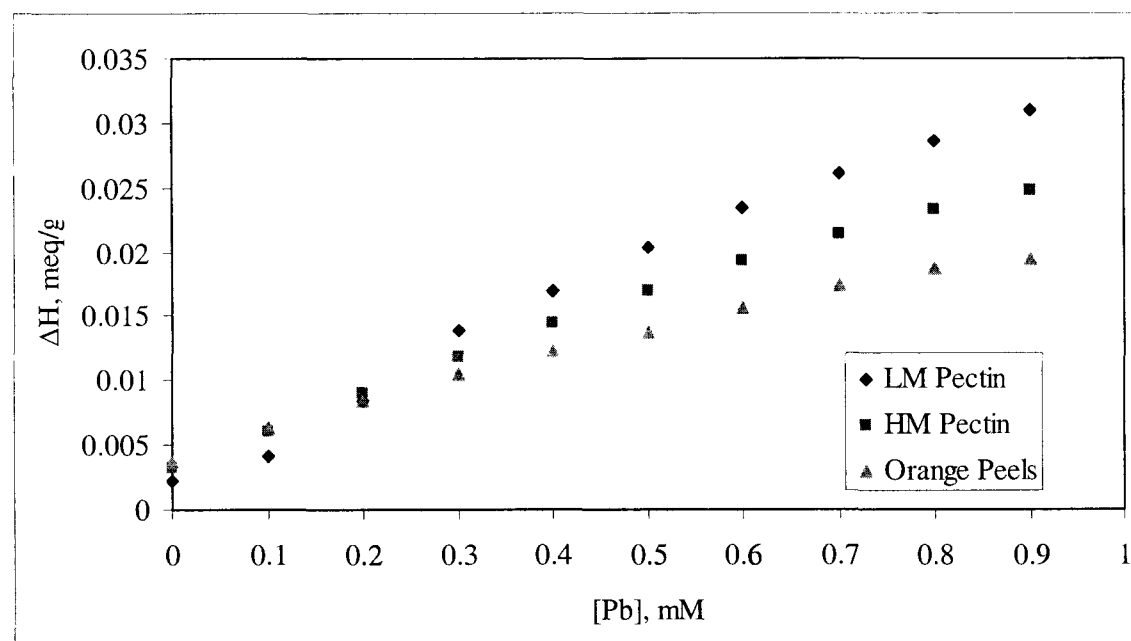


Figure 4.27:  $H^+$  released ( $\Delta H$ ) on incremental addition of Pb to the sorbent solution

#### 4.2.5 Spectroscopic Studies

Molecular scale analyses of samples after sorption (Pb-HM pectin, Pb-LM pectin, and Pb-peels) were conducted using Fourier Transform Infrared Spectroscopy (FTIR). Figures 4.28, 4.29, and 4.31 represent the respective results. A close analysis of these curves revealed that the absorption peak corresponding to the carboxylic (-COOH) groups shifted significantly from  $1627\text{ cm}^{-1}$  to  $1636\text{ cm}^{-1}$  in the case of HM pectin after treatment with Pb. A similar shift in the same peak from  $1624\text{ cm}^{-1}$  to  $1635\text{ cm}^{-1}$  could be observed for LM pectins as well. This shift in wave number corresponds to a change in energy corresponding to the functional group, which further reflects that the bonding pattern of carboxylic groups changes after sorption. This result confirmed the involvement of carboxylic groups in binding of Pb in the case of pectin. No significant shift in the peak corresponding to the ester group (-COOR) was observed in either case, which obviated any de-esterification for the given conditions. Furthermore, there was an additional peak at a value of  $1384\text{ cm}^{-1}$  in both cases, which was probably due to new bond formation that might correspond to the bond between Pb and the carboxylic groups of pectin.

Although the shift in the carboxylic acid peak was not significant in orange peels infrared spectra ( $1635\text{ cm}^{-1}$  compared to  $1638\text{ cm}^{-1}$ ), a similar new peak at a value of  $1382\text{ cm}^{-1}$  appeared after Pb sorption, suggesting a similar new bond formation. The shift of the carboxylic acid group might not be significant in this case because these groups were already at a higher energy level with an initial wave number of  $1638\text{ cm}^{-1}$ . This higher

energy level could be due to naturally present Ca bound to the carboxylic acid groups, which were later replaced by Pb ions. Binding experiments with a lower concentration (0.01 mM Pb) were also conducted to investigate whether the Pb concentration has any significant impact on the binding patterns and the size of new peak around  $1383\text{ cm}^{-1}$ , but the results were found to be similar, disproving that hypothesis (Figure 4.31). Binding of Pb with protonated peels also resulted in shift of the  $\text{-COOH}$  peak to a higher value, leading to similar binding mechanism (Figure 4.30). A comparison of the peels' spectra with the pectin spectra leads to the conclusion that carboxylic acid groups which are likely responsible for binding Pb by orange peels, which is consistent the second hypothesis.

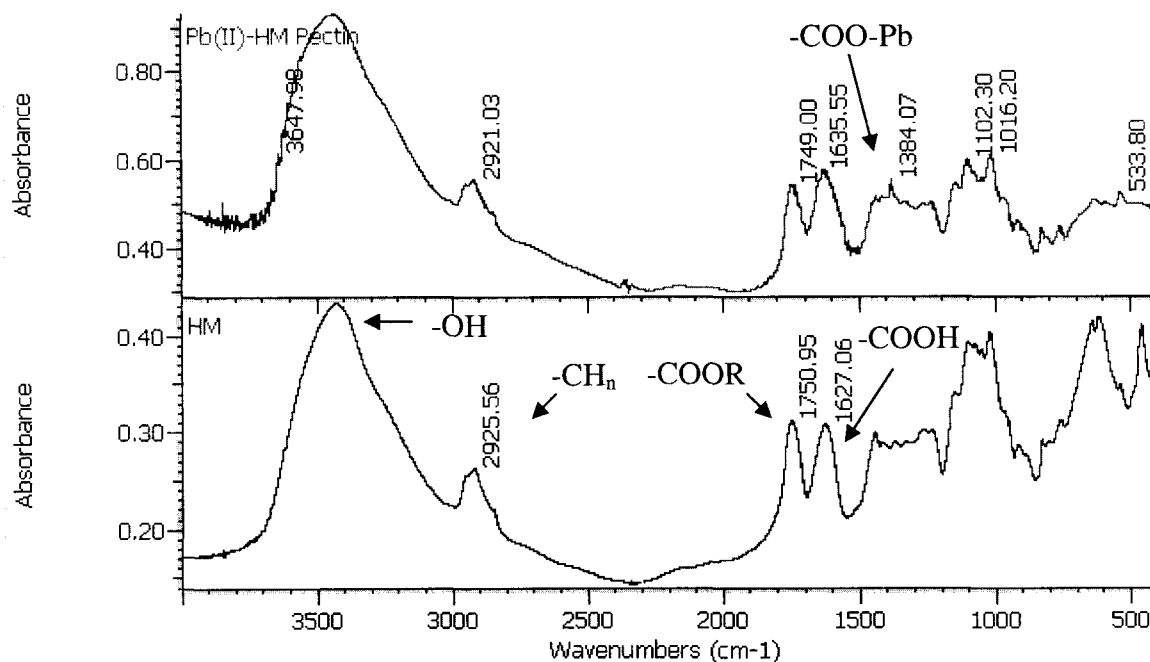


Figure 4.28: FTIR results for Pb binding by HM pectin

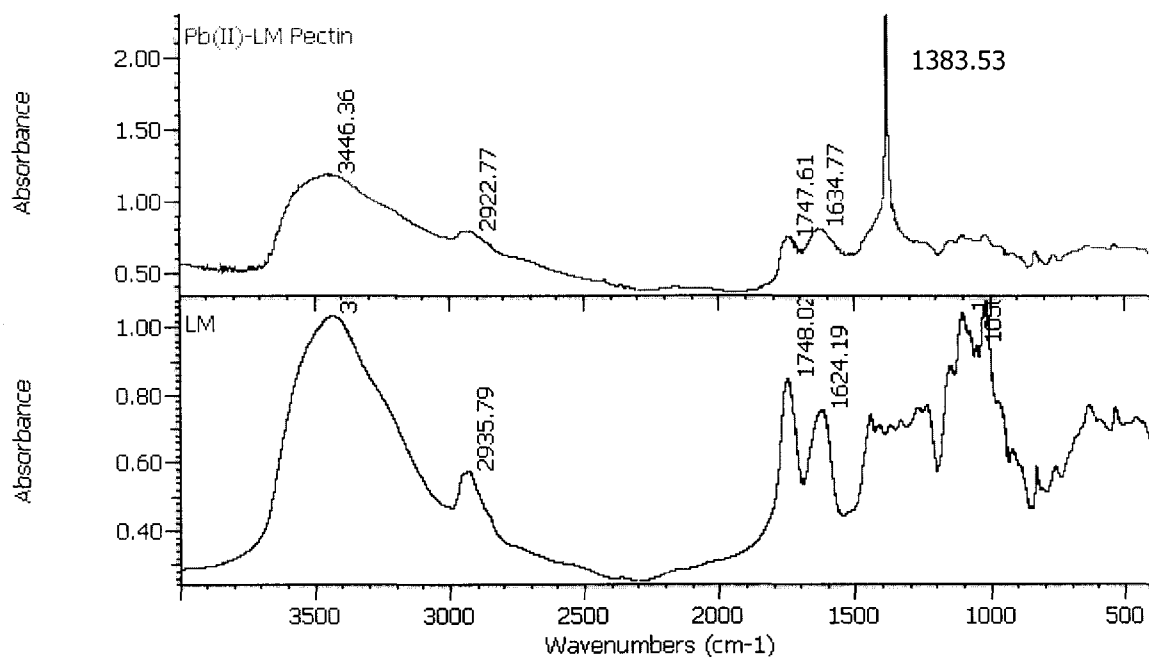


Figure 4.29: FTIR results for Pb binding by LM pectin

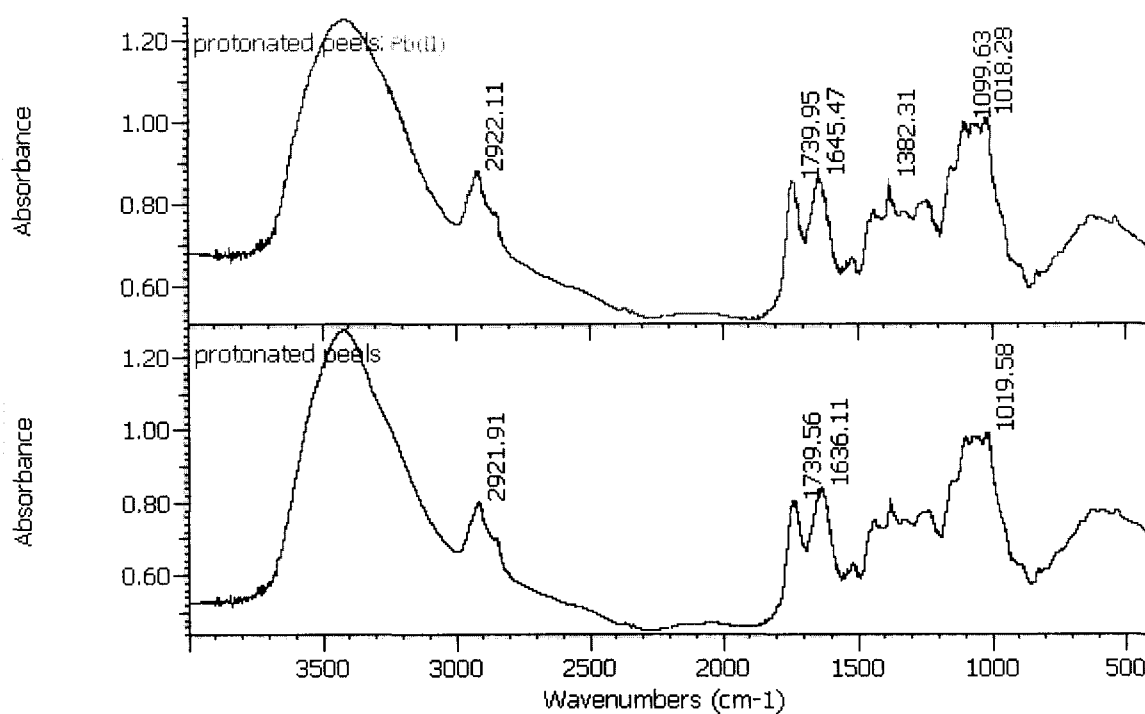


Figure 4.30: FTIR results for Pb binding by protonated orange peels

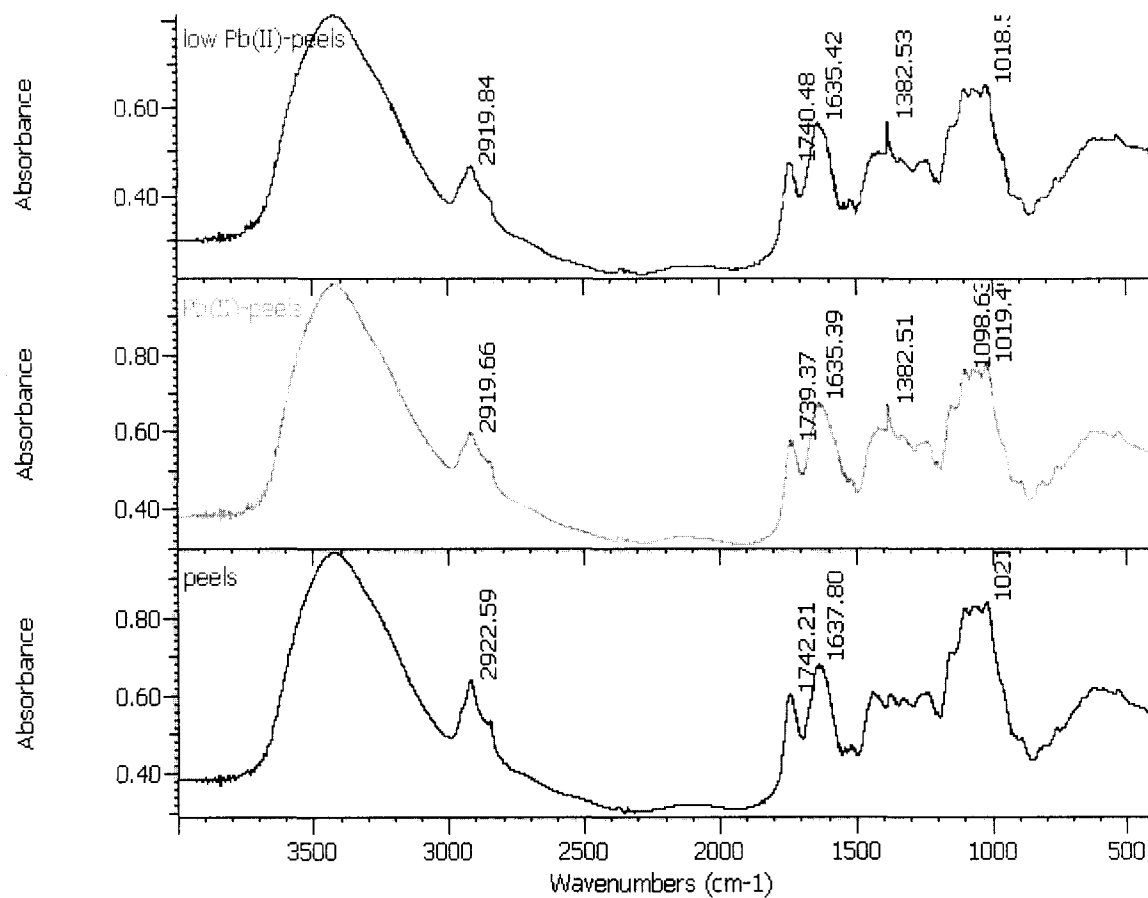


Figure 4.31: FTIR results for Pb binding by orange peels at different Pb concentrations:

0.1 mM Pb-peels (Pb(II)-peels) and 0.01 mM Pb-peels (low Pb(II)-peels)

## Chapter 5

### Conclusions and Recommendations

#### 5.1 Conclusions

From the studies conducted for this research work, the following conclusions can be drawn:

- The degree of methoxylation affects the net surface charge of citrus pectin, with higher surface charge present in low methoxylated pectin.
- Citrus pectin and peels have similar surface functional groups (especially carboxylic acid groups), confirming that pectin is an important component in orange peels that contributes to biosorption.
- Biosorption of Pb by citrus pectin and orange peels is fast, with equilibrium reached in less than 60 minutes, and it follows pseudo second-order kinetics.
- Pb uptake by orange peels depends on pH, ionic strength, and presence of co-ions but the impact of these parameters depends on sorbent dosage.
- Non-linear fitting of the Langmuir and Freundlich isotherms provides better fit than linear fitting for Pb biosorption by orange peels.
- The highest measured Pb uptake by orange peels was 1.93 mmol/g. However, no plateau value was reached for that concentration. The maximum uptake capacity according to the Langmuir model was 3.18 mmol/g or 658 mg/g, which is similarly high as for some ion exchange resins, consistent with the first hypothesis.

- Carboxylic groups are responsible for binding of Pb by citrus pectin as well as peels, and the second hypothesis holds as well.

Overall, present studies suggest that biosorption of Pb ions by orange peels can be a cheap and effective way of metal ion treatment and must be investigated further for its practical application.

## **5.2 Recommendations for Future Work**

Based on the present experiments and analyses, it is evident that orange peels can be a potential low cost biosorbent for removal of lead from aqueous solution. In order to extend the present study to practical applications, the following research can be recommended:

- Sorbent modification for strengthening the orange peels.
- Kinetic studies in sorption columns with continuous flow, including study of the effects of flow rates.
- Binary and multi-metal isotherm studies.
- Desorption and regeneration studies.

## References

**Agency for Toxic Substances and Disease Registry (ATSDR).** 2005. Toxicological profile for lead. (*Draft for Public Comment*). Atlanta, GA: U.S. Department of Health and Human Services, Public Health Service.

**Ajmal, M.; Khan-Rao R. A.; Ahmad, R.; Ahmad, J.** (2000) Adsorption studies of *Citrus reticulata* (fruit peel of orange): removal of Ni (II) from electroplating wastewater. *Journal of Hazardous Materials*. 79(1-2), 117-131.

**Aldor, I.; Fourest, E.; Volesky, B.** (1995) Desorption of cadmium from algal biosorbent. *Canadian Journal of Chemical Engineering*. 73(4), 516-522.

**Allison, J. D.; Brown, D. S.; Novo-Gradac, K. J.** *MINTEQ2/PRODEFA2: A Geochemical Assessment Model for Environmental Systems*; Center for Exposure Assessment Modeling, U.S. EPA: Washington, DC 1991.

**Annadurai, G.; Juang, R. S.; Lee, D. J.** (2003) Adsorption of heavy metals from water using banana and orange peels. *Water Science and Technology*. 47, 185-190.

**Antunes, W. M.; Luna, A. S.; Henriques, C. A.; da Costa, A. C. A.** (2003) An evaluation of copper biosorption by a brown seaweed under optimized conditions. *Journal of Biotechnology*. 6 (3), 1-11.

**Atkinson, B. W.; Bux, F.; Kasan, H. C.** (1998) Considerations for application of biosorption technology to remediate metal-contaminated industrial effluents. *Water South Africa*. 24 (2), 129-126.

**Balaria, A.; Schiewer, S.; Trainor, T.** (2005) Biosorption of Pb(II) onto Citrus Pectin: Effect of Process Parameters on Metal Binding Equilibrium and Kinetics *EWRI 2005: Impacts of Global Climate Change*, Anchorage, AK, May 2005.

**Chen, J.P.; Wang, L.** (2001) Characterization of a Ca-alginate based ion-exchange resin and its applications in lead, copper, and zinc removal. *Separation Science & Technology*. 36(16), 3617–3637.

**Cohen-Shoel, N.; Ilzyer, D.; Gilath, I.; Tel-Or E.** (2002) The involvement of pectin in Sr<sup>2+</sup> biosorption by Azolla. *Water Air and Soil Pollution*. 125 (1-4), 195-205.

**Copikova, J.; Synytsya, A.; Cerna, M.; Kaasova, J.; Novotna, M.** (2001) Application of FT-IR spectroscopy in detection of food hydrocolloids in confectionery jellies and food supplements. *Czech Journal of Food Sciences*. 19(2), 51-56.

**Cossich, E. S.; Tavares, C. R. G.; Ravagnani, T. M. K.** (2002) Biosorption of chromium (III) by *Sargassum sp.* biomass. *Journal of Biotechnology*. 5(2), 133-140.

**Davis, T.A.; Volesky, B.; Alfonso, M.** (2003) A review of the biochemistry of heavy metal biosorption by brown algae. *Water Research*. 37, 4311-4330.

**Debbaudt, Adriana; Zalba, Marta; Ferreira, M. L.; Gschaidner, M. E.** (2001) Theoretical and experimental study of  $Pb^{2+}$  and  $Hg^{2+}$  adsorption on biopolymers, 2. Experimental part. *Macromolecular Bioscience*. 1(6), 249-257.

**Dronnet, V.M.; Axelos, M. A. V.; Renard, C. M. G. C.; Thibault, J.F.** (1996) Characterization and selectivity of divalent metal ion binding by citrus and sugar beet pectin. *Carbohydrate Polymer*. 30, 253-263.

**Dronnet, V. M.; Renard, C. M. G. C.; Axelos, M. A. V.; Thibault, J. F.** (1997) Binding of divalent metal cations by sugar-beet pulp. *Carbohydrate Polymers*. 34(1-2), 73-82.

**Ferreira, M. L.; Gschaider, M. E.** (2001) Theoretical and experimental study of Pb<sup>2+</sup> and Hg<sup>2+</sup> adsorption on biopolymers, 1. Theoretical study. *Macromolecular Bioscience*. 1(6), 233-248.

**Genialab** (2002). Website of the Genialab Company on pectin properties and sources:

<http://www.genialab.de/inventory/pectinate.htm>.

**Gerente, C.; du Mesnil, P. C.; Andres, Y.; Thibault, J. F.; Le Cloirec, P.** (2000) Removal of metal ions from aqueous solution on low cost natural polysaccharides. Sorption mechanism approach. *Reactive & Functional Polymers*. 46(2), 35-144.

**Gloaguen, V.; Morvan, H.** (1997) Removal of heavy metal ions from aqueous solution by modified barks. *Journal of Environmental Science and Health, Part A: Environmental Science and Engineering & Toxic and Hazardous Substance Control*. A32(4), 901-912.

**Gnanasambandam, R.; Proctor, A.** (1999) Determination of pectin degree of esterification by diffuse reflectance Fourier Transform Infrared Spectroscopy. *Food Chemistry*. 68(3), 327-332.

**Grandjean, P.** (1975) Lead in Danes. Historical and Toxicological Studies, in *Environmental Quality and Safety, Suppl. Vol II, Lead*, (ed. F. Coulston and F. Korte), Academic Press, New York, San Francisco, London, pp. 6-75.

**Grant, G. T.; Morris, E. R.; Rees, D. A.; Smith, P. J. C.; Thom, D.** (1973) Biological interactions between polysaccharides and divalent cations: The egg-box model. *FEBS Letters*. 32, 195-198.

**Harel, P.; Mignot, L.; Sauvage, J. P.; Junter, G. P.** (1998) Cadmium removal from dilute aqueous solution by gel beads of sugar beet pectin. *Industrial Crops and Products*. 7, 239-247.

**Harrison R. M.; Laxen D. P. H.** (1981) Lead Pollution: Causes and Control. Chapman and Hall, London, New York.

**Hashim, M. A.; Chu, K. H.** (2004) Biosorption of cadmium by brown, green, and red seaweeds. *Chemical Engineering Journal (Amsterdam, Netherlands)* 97(2-3), 249-255.

**Henderson, J.; Baully, J. M.; Ashford, D. A.; Oliver, S. C.; Hawes, C. R.; Lazarus, C. M.; Venis, M. A.; Napier, R. M.** (1997) Retention of maize auxin-binding protein in the endoplasmic reticulum. Quantifying and the role of auxin. *Planta*. 202(3), 313-323.

**Inoue, K.; Ghimire, K. N.; Zhu, Y.; Yano, M.; Makino, K.; Miyajima, T.** (2002) Effective use of orange juice residue for removing heavy and radioactive metals from environments. *Geosystem Engineering*. 5(2), 31-37.

**Jumle, R.; Narwade, M. L.; Wasnik, U.** (2002) Studies in adsorption of some toxic metal ions on *Citrus sinensis* skin and *Coffea arabica* husk: Agricultural by product. *Asian Journal of Chemistry*. 14, 1257-1260.

**Kartel, M. T.; Kupchik, L. A.; Veisov, B. K.** (1999) Evaluation of pectin binding of heavy metal ions in aqueous solutions. *Chemosphere*. 38, 2591-2596.

**Kohn, R.** (1987) Binding of divalent cations to oligomeric fragments of pectin. *Carbohydrate Research*. 160, 343-353.

**Lee, S. H.; Shon, S. J.; Chung, H.; Lee, M.-Y.; Yang, J.-W.** (1999) Effect of chemical modification of carboxyl groups in apple residues on metal ion binding. *Korean Journal of Chemical Engineering*. 16, 576-580.

**Lee, S. H.; Yang, J.-W.** (1997) Removal of copper in aqueous solution by copper waste. *Separation Science and Technology*. 32(8), 1371-1387.

**Low, K. S.; Lee, C. K.** (1987) A comparative study of methods for the analysis of lead in mosses. *Pertanika* 10(2), 253-256.

**Maranon, E.; Sastre, H.** (1992) Behavior of lignocellulosic apple residues in the sorption of trace metals in packed beds. *Reactive Polymers*. 18, 173-176.

**Marshall, W. E.; Champagne, E. T.; Evans, W. J.** (1993) Use of rice milling byproducts (hulls and bran) to remove metal ions from aqueous solution. *Journal of Environmental Science and Health, Part A: Environmental Science and Engineering* A28(9), 1977-1992.

**Monsoor, M. A.; Kalapathy, U.; Proctor, A.** (2001) Improved method for determination of pectin degree of esterification by diffuse reflectance Fourier Transform Infrared Spectroscopy. *Journal of Agricultural and Food Chemistry* 49(6), 2756-2760.

**Pandey, S. S.; Thakkar, N. V.** (2004) Synthesis, characterization and applications of a new chelating resin containing nitrosocatechol. *Journal of Scientific & Industrial Research*. 63(8), 682-688.

**Panganelli, F.; Papini, P. M.; Toro, M.; Veligo, F.** (2000) Biosorption of metal ions on *Arthrobacter sp.*: Biomass characterization and biosorption modeling. *Environmental Science & Technology*.33, 2773-2778.

**Racape, E.; Thibault, J. F.; Reitsma, J. C. E.; Pilnik, W.** (1989) Properties of amidated pectins. II. Polyelectrolyte behavior and calcium binding of amidated pectins and amidated pectic acids. *Biopolymers*. 28(8), 1435-48.

**Reddad, Z.; Gerente, C.; Andres, Y.; Le Cloirec, P.** (2002) Modeling of single and competitive metal adsorption onto a natural polysaccharide. *Environmental Science & Technology*. 36(10), 2242-2248.

**Say R.; Denizli A.; Andres, Y.; Arica, M. Y.** (2000) Biosorption of cadmium(II), lead(II) and copper(II) with the filamentous fungus *Phanerochaete chrysosporium*. *Bioresource Technology*. 76(2001), 67-70.

**Schiewer, S.; Volesky, B.** (1995) Modeling of the proton-metal ion exchange in biosorption. *Environmental Science & Technology*. 29, 3049-3058.

**Senthilkumaar, S.; Bharathi, S.; Nithyanandhi, D.; Subburam, V.** (2000) Biosorption of toxic heavy metals from aqueous solutions. *Bioresource Technology*. 75(2), 163-165.

**Sergushchenko, I. S.; Kovalev, V. V.; Bednyak, V. E.; Khotimchenko, Yu. S. A.** (2003) Comparative evaluation of the metal-binding activity of low-esterified pectin from the seagrass *Zostera marina* and other sorbents. *Russian Journal of Marine Biology (Translation of Biologiya Morya (Vladivostok, Russian Federation))*. 30(1), 70-72.

**Smith, S.D.; Ferris, G.F.** (2001) Proton binding by hydrous ferric oxide and aluminum oxide surfaces interpreted using fully optimized continuous  $pK_a$  spectra. *Environmental Science & Technology*. 35(23), 4637-4642.

**Stumm W.; Morgan J. J.** (1970), Aquatic Chemistry, Wiley-Interscience, A Division of John Wiley & Sons, Inc., New York.

**Synytsya, A.; Copikova, J.; Matejka, P.; Machovic, V.** (2003) Fourier transform Raman and infrared spectroscopy of pectins. *Carbohydrate Polymers*. 54 (1), 97-106.

**USEPA** (1999), Review of the National Ambient Air Quality Standards for Lead: Exposure Analysis Methodology and Validation. Office of air quality planning and standards. Research Triangle Park, North Carolina.

**Vincent** (2001) Website of Vincent Corporation on production of pectin peels. [http://www.vincentcorp.com/tech\\_papers/fmc2\\_sg.html](http://www.vincentcorp.com/tech_papers/fmc2_sg.html).

**Volesky, B.** (2003) Biosorption: Application aspects–process simulation tools. *Hydrometallurgy*. 71 (1-2), 179-190.

**Volesky, B.** (1999) Sorption and Biosorption - Chapter 6: Evaluation of biosorption performance. *ISBN 0-9732983-0-8*, 103-178.

**Volesky, B.** (1990). Biosorption of heavy metals. CRC Press Inc., Boca Raton, USA

**Yang, J. ; Volesky, B.** (1999) Biosorption and elution of uranium with seaweed biomass: *Biohydrometallurgy and the Environment Toward the Mining of the 21st Century*, International Biohydrometallurgy Symposium Proceedings, 1999, volume B, Ballester, A. & Amils, R. (eds.) Elsevier Sciences, Amsterdam, The Netherlands: pp.483-492.

**Yang, M.; Fu, Y.; Huang, N.** (2004) Study on adsorption properties of ion exchange resin containing ether linkage for  $\text{Cu}^{2+}$  and  $\text{Pb}^{2+}$  *Hunan Keji Daxue Xuebao, Ziran Kexueban*. 19(3), 74-77

**Yano, M.; Inoue, K.** (1997) Adsorption of metal ions on alginic acid amide, pectic acid amide, crosslinked pectic acid and crosslinked alginic acid. *Analytical Sciences*. 13 (Suppl., Asianalysis IV), 359-360.

**Yun, Y-A.; Park, D.; Park J. M.; Volesky, B.** (2001) Biosorption of trivalent chromium on the brown seaweed biomass. *Environmental Science & Technology*. 35, 4353-4358.

## Appendix A

### List of Symbols and Acronyms

$\theta$	Langmuir equilibrium adsorption constant in L/meq of Pb
$\eta$	Freundlich constant related to adsorption capacity
$C$	Coulomb
$C_e$	Final concentration in meq of Pb /L
$eq$	equivalents
$HM$	High methoxylated pectin
$I. S.$	Ionic Strength
$k_1$	First-order rate constant in $\text{min}^{-1}$
$k_2$	Second-order rate constant in $\text{g/meq-min}$
$k_f$	Freundlich constant related to intensity
$LM$	Low methoxylated pectin
$p$	Number of data points
$q$	Metal uptake in mmol of Pb/g sorbent
$q_e$	Equilibrium metal uptake in mmol of Pb / g sorbent
$q_{max}$	Maximum metal uptake in mmol of Pb / g sorbent
$SSE$	Average sum of squared errors
$S$	Net surface charge
$t$	Time interval in min

## Appendix B

## Preliminary Experimental Results

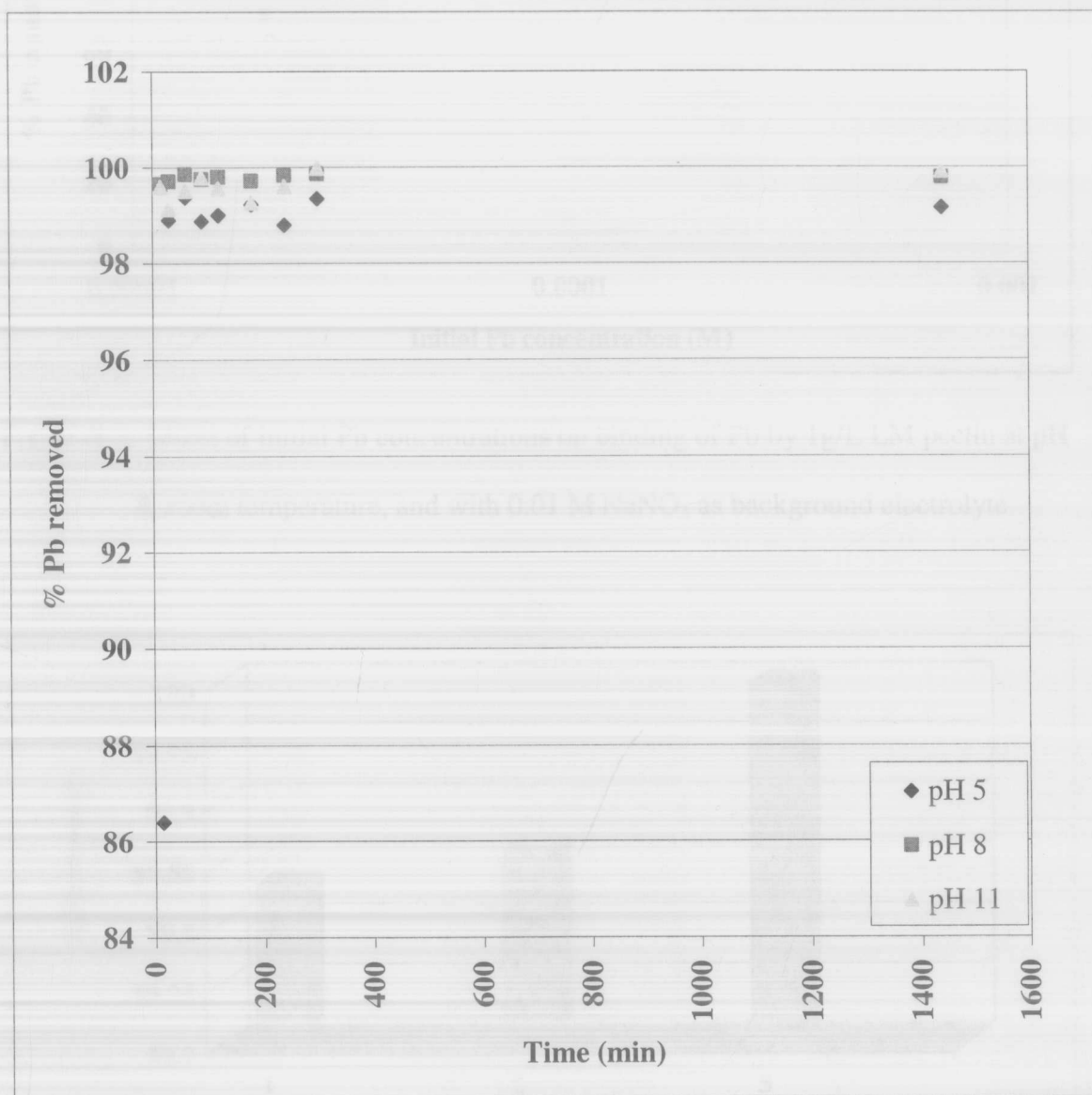


Figure B.1: Kinetics of binding of  $10^{-3}$  M Pb by 1g/L LM pectin at room temperature and with 0.01 M  $\text{NaNO}_3$  as background electrolyte

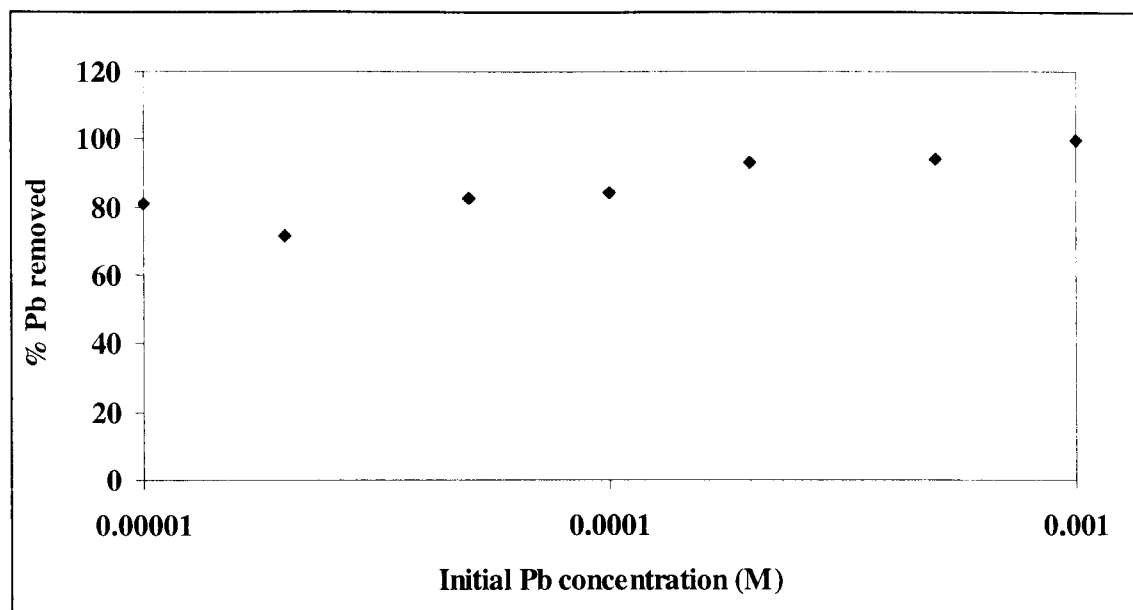


Figure B.2: Effect of initial Pb concentrations on binding of Pb by 1g/L LM pectin at pH 8, room temperature, and with 0.01 M NaNO<sub>3</sub> as background electrolyte

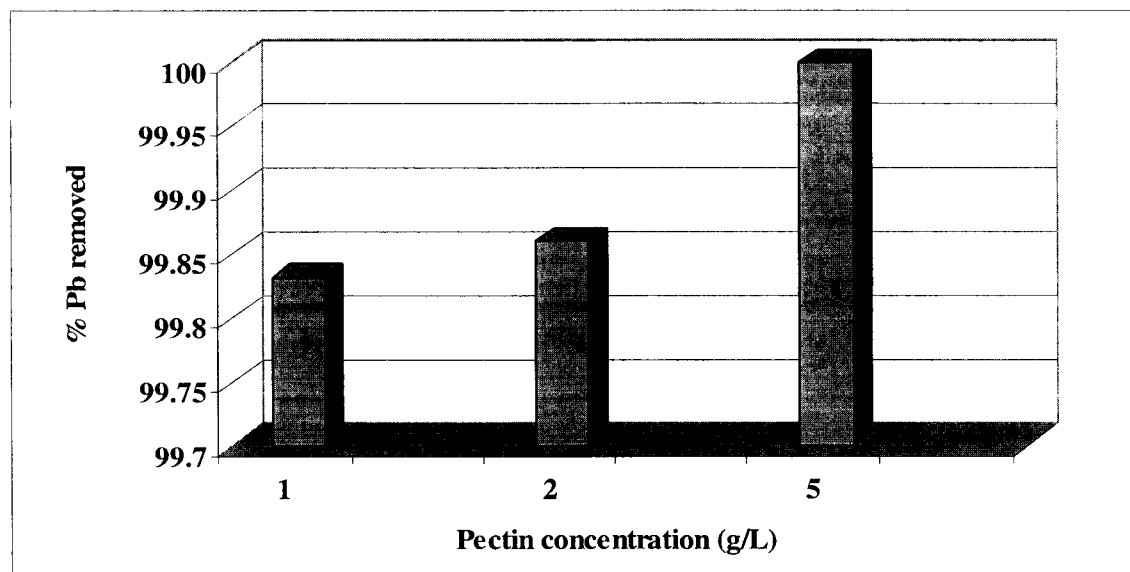


Figure B.3: Effect of pectin concentration on binding of 10<sup>-3</sup> M Pb by LM pectin at pH 8, room temperature, and with 0.01 M NaNO<sub>3</sub> as background electrolyte

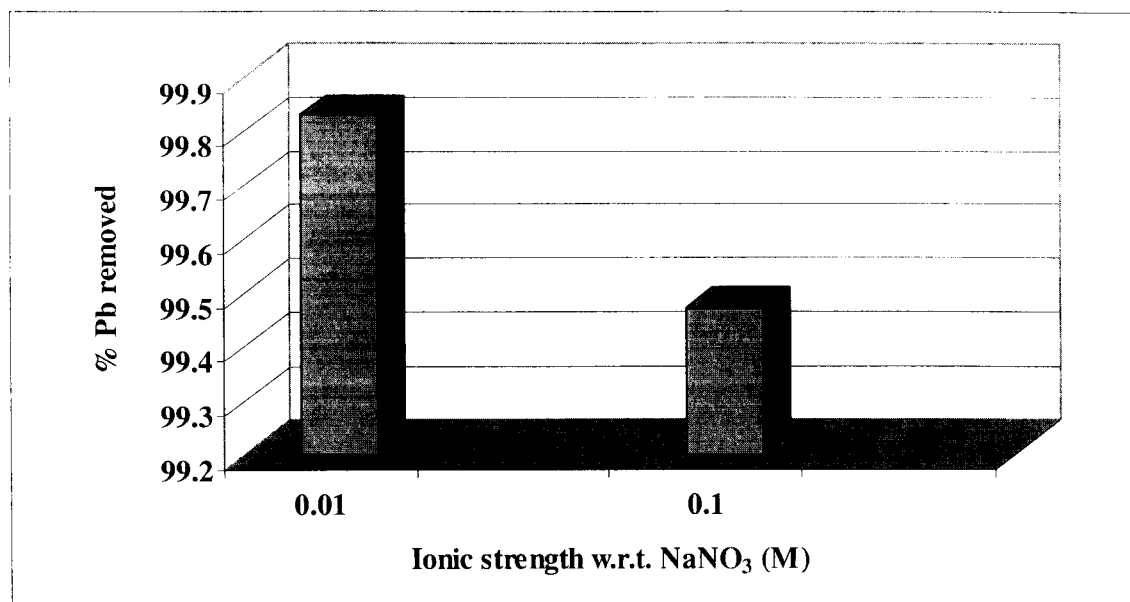


Figure B.4: Effect of ionic strength on binding of  $10^{-3}$  M Pb by 1g/L LM pectin at pH 8 and room temperature

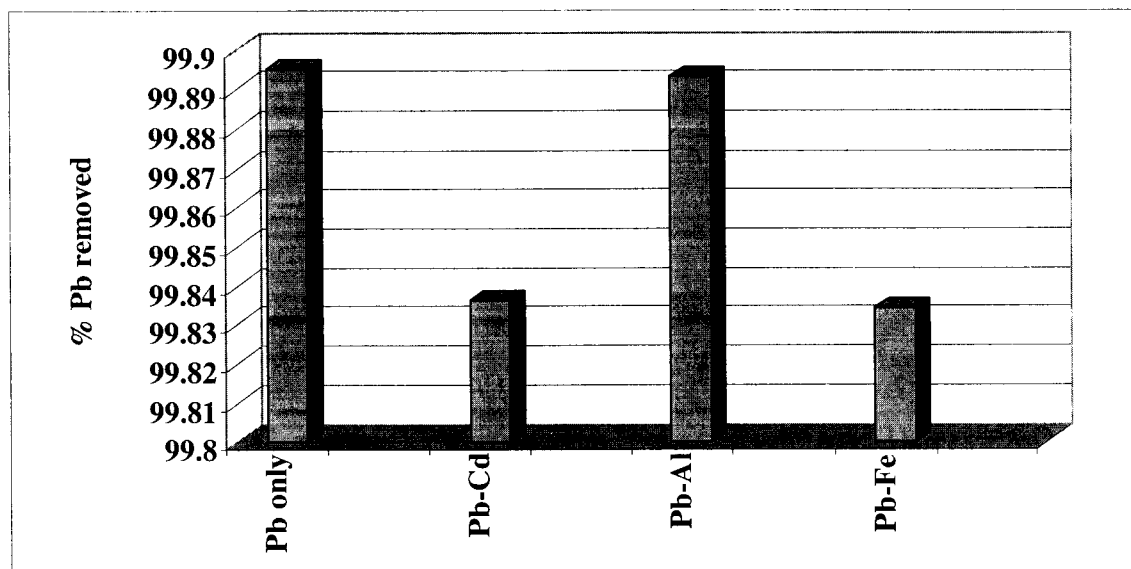


Figure B.5: Effects of presence of co-ions on binding of  $10^{-3}$  M Pb by 1 g/L LM pectin at pH 8, room temperature, and with 0.01 M NaNO<sub>3</sub> as background electrolyte

## Appendix C

### Duplicate Experiments and Sampling

Table C.1: Duplicate Experiments and Sampling

Sample ID	Type of Duplication	Concentration by GAA Spectrometer ppb	Dilution	Sample Concentration ppb	Relative Standard Deviation %
Isotherm: 50 mg/L	original	15.71	105	1649.55	7.06
	duplicate experiment	17.36	105	1822.8	
Isotherm: 200 mg/L	original	59.4	1640	97416	4.33
	duplicate experiment	55.87	1640	91626.8	
Environmental Conditions: pH 5 Limited Sorbent	original	68	205	13940	1.74
	duplicate sampling	66.35	205	13601.75	
Environmental Conditions: 0.1 M NaNO <sub>3</sub> , Limited Sorbent	original	10.2	205	2091	13.94
	duplicate sampling	8.37	205	1715.85	
Environmental Conditions: Co-ion Ca, Excess Sorbent	original	11.2	205	2296	3.76
	duplicate sampling	10.62	205	2177.1	